KINETIC STUDY OF NIOBIUM OXYCHLORIDE CHLORINATION IN A FLOW REACTOR BY SEQUENTIAL STATISTICAL DESIGN

by

Robert Jost Graham

A Dissertation Submitted to the
Graduate Faculty in Partial Fulfillment of
The Requirements for the Degree of
DOCTOR OF PHILOSOPHY

Major Subject: Chemical Engineering

Approved:

Signature was redacted for privacy.

In Charge of Major Work

Signature was redacted for privacy.

Head of Major Department

Signature was redacted for privacy.

Dean of Graduate College

Iowa State University
Of Science and Technology
Ames, Iowa

1970

TABLE OF CONTENTS

I. INTRODUCTION

Niobium and nonferrous-niobium-base alloys, although of no commercial importance until the 20th century, now find many applications in the atomic, aircraft and space industries. Niobium is used in the atomic energy field because of its high melting point, good high temperature strength, low neutron absorption cross section, excellent corrosion resistance to acids, and suitable physical and mechanical properties that make niobium an excellent clading material for nuclear fuels. Niobium high temperature alloys also find many applications for jet engines, gas turbines, high speed air craft and missiles. As a result of the increasing number of applications for niobium, more research is needed in the field of production and refining of niobium metal. This work is concerned with one aspect of the production of pure niobium metal.

The production of pure niobium metal by the process of chlorinating the ores, separating the $NbCl_5$ from other metal chlorides, and reducing the $NbCl_5$ to pure niobium metal appears to be an economically attractive and practical method (6, 19, 27, 38). A troublesome impurity that occurs at various stages in this method is niobium oxychloride ($NbOCl_3$). $NbOCl_3$ is formed along with niobium pentachloride ($NbCl_5$) during the chlorination of the ores and during subsequent operations by the reaction of $NbCl_5$ with moisture and oxides. If present during the reduction step, the $NbOCl_3$ is reduced to niobium oxides which greatly reduce the quality of the metal product.

One method of eliminating $NbOCl_3$ is by chlorinating it with phosgene ($COCl_2$) to form $NbCl_5$ (6, 13, 18). Boesiger (7) pointed out the advantages of this method and suggested rate equations to represent the kinetics

of the reaction. A principal goal of this research was to determine if the models proposed by Boesiger or some other model would adequately represent the chlorination of $NbOCl_3$ with $COCl_2$, particularly at low $NbOCl_3$ concentrations at which the $NbOCl_3$ impurity would generally be encountered. A second goal was to determine the parameters of the best model as accurately as possible.

As is often the case with kinetic experiments, the experimenter cannot tell what experiments are needed until at least some experiments are completed. This suggests an iterative approach consisting of performing an experiment, analyzing the data, and using the results to determine the next experiment. Box and Hunter (10, 11) have clearly described this sort of iterative ppproach.

Since the experiments were difficult to perform and time consuming, it was desirable to set up an experimental design which would produce the necessary data for precise parameter estimates in as few experiments as possible. Therefore, the experimental design was based on a criterion suggested by Box et al. (8, 10, 11, 12) which chooses the experimental conditions that minimize the volume of the joint confidence region of the parameters. The ability of this criterion to obtain precise parameter estimates in a few experiments has been demonstrated by several authors (25, 26, 29).

A third goal was to analyze the experimental design and to examine the effect of the size of the experimental error on the accuracy and convergence of the parameter estimates at each stage of the experimental design.

II. PREVIOUS WORK

Chlorination of $NbOCl_3$ has been reported by several researchers as a means of eliminating $NbOCl_3$ from $NbCl_5$-$NbOCl_3$ mixtures. With the exception of Boesiger (7), however, these reports contain very little kinetic information.

Nisel'son (38) found $NbOCl_3$ could be converted to $NbCl_5$ by chlorination with carbon tetrachloride or thionyl chloride in a batch reactor. "Complete" conversion was attained in 5-8 minutes at temperatures of 330-350°C and pressures of 25-30 atm.

Elger and Boubel (19) patented a method for the production of hafnium which they claimed could also be used for other metals such as niobium. The method involved chlorinating mixed chlorides with chlorine gas as the mixture flowed through a graphite tube. The oxygen was removed in the form of carbon monoxide by reaction of the oxides with the graphite.

The conversion of $NbOCl_3$ to $NbCl_5$ by chlorination in a flow reactor with $COCl_2$ or a mixture of carbon monoxide and chlorine was reported by Dunn (17, 18). The reaction was carried out at 350-600°C in the presence of charcoal which reportedly acted as a catalyst.

Brothers (13) patented a method for preparation of charcoal for use in a continuous flow process. Good results were obtained for the chlorination of $NbOCl_3$ in a bed of the charcoal by using chlorine, carbon tetrachloride, or $COCl_2$ as chlorinating agents.

Boesiger (7) studied the chlorination of $NbOCl_3$ with $COCl_2$ using batch reactors. After considering several possible models, he found the following to best fit his data:

$$dC_A/dt = -kC_A^{\theta_3} C_B^{\theta_4} \quad .$$

The best estimates of θ_3 and θ_4 were 0.917 and 1.013, respectively. The specific reaction rate for the temperature range 360-450°C was:

$$k = 0.526 \times 10^6 \exp(-21{,}200/RT) \quad .$$

Boesiger's parameter estimates were relatively imprecise, and as a result, he made several suggestions for future work for better parameter estimation. Two of these suggestions were incorporated into this study. First gas chromatography was used as a more rapid and more accurate means of obtaining kinetic data. Second, an iterative statistical experimental design was used for planning the experiments.

The application of nonlinear estimation theory to the analysis of kinetic data has progressed rapidly with the development of modern, high speed computers. Nonlinear techniques have been developed which are used for parameter estimation, model discrimination, and experimental design.

An introduction to the basic theory of nonlinear estimation is presented in a text by Draper and Smith (16). Box (8) describes both linear and nonlinear techniques for fitting equations to experimental data. Examples of nonlinear estimation applied to parameter estimation and model discrimination have been reported (9, 30, 37, 39, 40). In some cases (28, 33) several models were found that fit the experimental data equally well, and no discrimination between the models was possible. Peterson and Lapidus (41) give an example where model discrimination was possible as the result of good experimental design.

The analysis of residuals is used frequently as a tool to determine the adequacy of models representing kinetic data (9, 28, 30, 31, 33). Confidence regions have been used to yield information about the precision

of the parameter estimates (1, 9, 11, 31, 37). Beale (2) gives a thorough treatment of confidence regions applied to nonlinear estimation.

Nonlinear estimation theory has been applied to the problem of experimental design only recently. Box (9), Box and Hunter (10, 11) and Box and Lucas (12) presented the methods which served as the basis of the experimental design in this study. Box and Hunter (11) suggested the use of an interative cycle for checking and modifying a model in which statistical analysis was applied to the estimated parameters to determine the source and nature of possible inadequacies.

Box (9) and Box and Lucas (12) suggested that the experimental design should be chosen to minimize the volume of the approximate confidence region of the parameters. Box and Hunter (10) used this experimental design criterion and an iterative cycle of four steps - conjecture, design, experimentation, and analysis - for estimation of the parameters of a kinetic model. The iterative cycle was employed in a sequential plan in which the parameters were reestimated at each stage, and the independent variables for the next stage were chosen according to the criterion of Box and Lucas (12). They demonstrated the feasibility of this approach by using a computer and a "true model" to generate data with a known normally distributed experimental error. A kinetic model with three parameters and two independent variables was assigned as the "true model".

In the same manner, Hunter and Atkinson (25) showed how eight experiments using the approach of Box and Hunter (10) produced parameter estimates with approximately the same degree of precision as an unplanned approach of 38 more or less random experiments. The usefulness of this approach was demonstrated in a similar manner by Kittrell et al. (29) and

Hunter et al. (25).

Behnken (3) applied the experimental design of Box and Lucas (12) to an actual chemical problem. The experimental design was used to select the setting of the independent variable (in this case the initial feed ratio) for two experiments which were used for estimating a copolymer reactivity ratio containing two parameters.

III. THEORY

A. Kinetic Models

One of the goals of this study was to determine if the kinetic model proposed by Boesiger (7) or some other kinetic model would represent the chlorination of $NbOCl_3$ with $COCl_2$ at low $NbOCl_3$ concentrations. Some prior information such as the stiochiometry, thermodynamic data, and thermal decomposition data of the reactants was available.

The conversion of $NbOCl_3$ to $NbCl_5$ by chlorination with $COCl_2$ is represented by the following stiochiometric equation:

$$NbOCl_3 + COCl_2 = NbCl_5 + CO_2 \qquad (1)$$

Calculations of the equilibrium constant, K, indicate this reaction is irreversible. Typical values of K are on the order of 10^6 - 10^7 between 500-350°C (6). These high values of the equilibrium constants suggest that the rate of reaction of $NbCl_5$ and CO_2 is negligible when compared to the rate of reaction of $NbOCl_3$ and $COCl_2$. Experimental work conducted by Boesiger (6) confirmed this assumption.

Thermal decomposition of $NbOCl_3$ is known to occur, requiring minor corrections to the initial concentrations of $NbOCl_3$. The thermal decomposition of $COCl_2$ was assumed to be negligible for the conditions of this study. Additional discussion of the $NbOCl_3$ and $COCl_2$ decomposition is found in Appendix A.

The general expression for the rate of chlorination of $NbOCl_3$ by $COCl_2$ may be represented by Model 1 as follows:

$$r = dC_A/dt = -kC_A^{\Theta_3} C_B^{\Theta_4} \qquad (2)$$

where:

r = rate of $NbOCl_3$ conversion, g moles/liter, sec.

t = residence time, seconds

k = specific rate constant in appropriate units

C_A, C_B = concentration of $NbOCl_3$ and $COCl_2$ respectively, in g moles/liter

Θ_3, Θ_4 = reaction order parameters

The specific rate constant, k, is assumed to be a function of temperature, T (°K), according to the Arrenhius equation:

$$k = A \exp(-E/RT)$$

where R is the ideal gas constant and A and E are frequency factor and activation energy, respectively.

The results of Boesiger's (7) work indicate that Model 1 adequately describes the kinetics of the reaction. Therefore, Model 1 was the principal model used throughout this study for the estimation of parameters and for the experimental design.

Other models derived from postulated mechanisms for the reaction were considered. These models were compared with Model 1 by examining the "goodness of fit" of the models to the data. Two of these models and their mechanisms are as follows:

Model 2

Mechanism: $NbOCl_3 + COCl_2 \rightarrow NbCl_5 + CO_2$

Rate Expression: $r = -kC_AC_B$

Model 3

Mechanism: $COCl_2 \underset{k_2}{\overset{k_1}{\rightleftharpoons}} COCl_2^*$

$$COCl_2^* + NbOCl_3 \xrightarrow{k_3} NbCl_5 + CO_2$$

$$dC_B^*/dt = 0$$

Rate Expression:

$$r = \frac{-kC_AC_B}{k'C_A + 1.0}$$

$$k = k_1k_3/k_2$$

$$k' = k_3/k_2$$

Model 2 is an elementary second order-irreversible reaction and is a special case of Model 1. Model 3 is based on the assumption of the formation of a transition type intermediate, essentially at a constant concentration (Steady State Assumption). This assumption is valid if the intermediate is very reactive and present at very small concentrations. There is no direct evidence of the existence of transition intermediates, but the assumption of their existence along with the steady state assumption provide simplifying assumptions that sometimes lead to useful kinetic models. Many other models based on transition intermediates could be developed. Model 3 is one of five of these models considered in this study.

B. The Method of Obtaining Data and Estimating Parameters

The steady state plug flow reactor method was chosen to obtain data to estimate the parameters A, E, θ_3, and θ_4 of Model 1. The method consists of allowing the reactants to flow at constant rates into one end of a long small diameter tube where the reactants mix and react at constant temperature and pressure as they pass through the tube. The composition of the material leaving the opposite end of the tube is then analyzed to determine the extent of the reaction.

The basic assumptions involved are the assumption of steady state and the assumption of plug flow. The steady state assumption is met if temperature, pressure, and flow rates are constant during the experiment. The necessary and sufficient conditions for plug flow is that the residence

time in the reactor is the same for all elements of fluid passing through the reactor. Levenspiel (34) and Cleland and Wilhelm (14) have developed criteria for estimating the degree to which the assumption of plug flow is met. The plug flow assumption can readily be justified by criterion of either author for the conditions and reactor dimensions used in this study (Refer to Appendix B).

The plug flow reactor method has several advantages over the constant volume reactor method. For example, the plug flow reactor method allows the use of quick, accurate gas chromatograph measurements compared to slow, complicated analytical techniques required for the constant volume type reactor method. Also, the operation of the $NbOCl_3$ sublimer of the plug flow reactor method eliminates the need for complicated purification or analysis of $NbOCl_3$.

On the basis of the plug flow assumption, the following differential equation accounts for the moles of $NbOCl_3$ reacting in a differential section of the reactor:

$$-rdV = F_o dx \qquad (3)$$

where:

x = g moles $NbOCl_3$ reacting/g moles $NbOCl_3$ flowing into the reactor

F_o= g moles $NbOCl_3$ fed to the reactor, g moles/sec

V = volume of the reactor, liters

r = rate at which $NbOCl_3$ reacts, g moles/liter sec

Integration of Equation 3 under steady flow conditions leads to:

$$V/F_o = \int_0^{x_f} dx/(-r) \qquad (4)$$

where:

x_f = x at reactor outlet.

Equation 4 can be written in a more useful form by the appropriate substitutions of the following relationships:

$$\tau = C_{Ao}V/F_o$$

$$C_A = C_{Ao}(1-x)$$

$$C_{Af} = C_{Ao}(1-x_f)$$

$$dC_A = -C_{Ao}dx$$

where:

C_{Ao} = initial concentrations of $NbOCl_3$, g moles/liter

C_A = concentration of $NbOCl_3$, g moles/liter

C_{Af} = concentration of $NbOCl_3$, g moles/liter, at reactor outlet

τ = space time, seconds

Substituting these equations into Equation 4 plus the substitution of Equation 2 for r gives:

$$\tau = \int_{C_{Ao}}^{C_{Af}} \frac{dC_A}{A \exp(-E/RT)\, C_A^{\Theta_3} C_B^{\Theta_4}} \qquad (5)$$

Integration may be accomplished by a fourth order Runge-Kutta numerical technique. For the special case of θ_3 and θ_4 equal to unity, Equation 5 can be integrated analytically.

Since the conversion cannot be measured directly, y, the mole ratio of CO_2 to the total moles of noncondensible gases (Ar, CO_2, $COCl_2$) from the reactor was used as a measure of the extent of the reaction. The quantity, y, designated as the observed response, was measured directly by the chromatograph.

The estimated mole ratio of CO_2 to the noncondensible gases from the reactor, $\hat{y}$, was calculated by the equation:

$$\hat{y} = (C_{Ao}-C_{Af})/C'_{Total} \qquad (6)$$

where C_{Af} was calculated from Equation 5 and C'_{Total} is the concentration of $COCl_2$, Ar and CO_2 from the reactor evaluated at the reactor temperature and pressure. The quantity, $\hat{y}$, is called the predicted response.

After values of y have been obtained experimentally, the problem is to find estimates for the parameters of Model 1 which produce values of $\hat{y}$ which best approximate y. The estimates of the parameters were obtained by the method of nonlinear least squares. The details of this method have been published previously (6) and are discussed in Appendix C.

With the estimates of the parameters, the adequacy of fit of the proposed model and the precision of the parameter estimates can be obtained by comparisons of the sum of squares of the residuals, F tests, and analysis of the residuals. Approximate estimates of confidence regions and confidence intervals of the parameters are useful in determining the precision of the parameters. These tests of the adequacy of fit and precision are discussed further in Appendix D.

C. Experimental Design

Determination of the settings of the independent variables is the objective of the experimental design. The experimental design should choose the variable settings such that (a) precise and accurate estimates of the parameters are obtained in an efficient manner and (b) the model is tested to determine if the model adequately describes the reaction over the range of independent variables.

The experimental design of this study was previously described by Box and Hunter (10) and consists of sequentially picking the best set of operating conditions for the next run, conducting the experiment, and reevaluating

the parameter estimates from the new data and the data of all the preceding experiments. Iteration of this sequence is carried out until the parameters have been accurately determined, and the model has been established.

The iterative procedure is extremely adaptable and modifications can be made at any stage. For instance, Model 1 may not adequately fit the data. In this case, the model may be modified or replaced by a new model suggested by the data or an examination of s_e^2 may indicate that a weighted least squares analysis is necessary.

The first step in the experimental design is to determine practical limits for the levels of the independent variables. In practice, there are maximum and minimum levels of the independent variables that define an experimental region or sample space in which experiments can be performed. For instance, the minimum $COCl_2$ and argon flow rates are defined by the lowest rates the flow meters can measure accurately. Details on how these limits were chosen in this work are found in Appendix E.

Once the experimental region for the independent variables has been defined, one must choose a criterion for deciding where in this region data will be taken. The criterion must select the settings of the independent variables so that the experiments will provide the estimates of the parameters accurately and efficiently. In addition, the experiments should adequately test the model. That is, the experiments should answer such questions as: "Does the model predict as well at high temperatures as at low temperatures?", "Under what conditions does the model fail?" etc.

The primary criterion which was used for selecting the conditions for the experimental runs is referred to as the Δ (del) criterion. The Δ criterion should provide accurate estimates in an efficient manner, but the Δ

criterion may not adequately test the model. For this reason, additional experiments may be required to test the model.

The Δ criterion requires data from at least four runs to begin. After the initial experimental runs have been completed and the parameters have been estimated by nonlinear least squares, the experimental conditions for the next experimental run must be chosen. To meet the Δ criterion, the settings of the independent variables for the next run are chosen to maximize the quantity, Δ.

The quantity, Δ, is defined as the determinant of the G^TG matrix. Here, G is the matrix defined in Equation 7 and G^T is simply the transpose of G:

$$G = \begin{bmatrix} g_{1,1} & g_{1,2} & \cdots & g_{1,p} \\ g_{2,1} & g_{2,2} & \cdots & g_{2,p} \\ \vdots & & & \vdots \\ g_{N,1} & g_{N,2} & \cdots & g_{N,p} \\ g_{N+1,1} & g_{N+1,2} & \cdots & g_{N+1,p} \end{bmatrix} \qquad (7)$$

where:

N = Number of previous runs

p = Number of parameters

g_{uj} = Partial derivative of y with respect to the j^{th} parameter at the u^{th} set of experimental conditions and the set parameters determined after the N^{th} experiment.

In this way the parameter estimates of the first N runs were used to determine the experimental conditions for the next run.

The rationale for the use of the Δ criterion has been discussed by Box and Lucas (12) and Hunter and Atkinson (25). For a linear model, the boundary of the $1 - \alpha$ joint confidence region is given by values of the parameters, $\vec{\theta}$, which satisfy:

$$(\vec{\theta} - \hat{\theta})[G^T G](\vec{\theta} - \hat{\theta}) = ps^2 F(p, N - p, 1 - \alpha)$$

where:

$\hat{\theta}$ = set of parameter estimates which minimize the sum squares of the residuals

s^2 = mean square about the regression

F = the F distribution with p and N - p degrees of freedom at the significance level.

For a nonlinear model, the above relationship is not strictly true. However, if the experimental errors are approximately normally distributed and the predicted response relationship is approximately linear in the vicinity of $\hat{\theta}$, then the volume of the joint confidence region is approximately proportional to the square root of the inverse of the determinant, Δ. A small volume of the joint confidence region represents precise estimates of the parameters. Therefore, on completion of the N^{th} run, the choices of the independent variables for the next run should be the ones which maximize Δ; that is, minimize the joint confidence region.

The method of obtaining the settings of the five independent variables (volume of the reactor, temperature, and the flow rates of argon, $COCl_2$, and $NbOCl_3$) which maximize Δ requires some discussion. A grid type search method was employed to determine these settings.

Two types of grids were used. The first, designated as the "coarse grid", was used to scan the Δ surfaces to see if there were any unusual features. The principal function of these grids was to determine if any general trends could be seen such as high Δ's at high $NbOCl_3$ flow rates or high Δ's at large reactor volumes.

A coarse grid was constructed for 24 combinations of the flow rates of $COCl_2$, Ar, and $NbOCl_3$ within the practical flow rate limits. Each grid was constructed using the temperature in 25°C increments in the range 325-475°C as the Y axis, and the reactor volume in 50 cc increments in the range 50-350 cc as the X axis. The value of Δ was then calculated at each point of the grid except at points where the limits of the sample space were violated.

The second grid was designated as the "fine grid". The ordinate was constructed using the temperature in 10°C increments in the range 340-460°C. The abscissa consisted of only two volumes (the actual volumes of the two reactors -- 72 cc and 340 cc). Grids were constructed for 39 different flow rate combinations. In general these flow rates were chosen in areas that indicated high Δ's from the "coarse grid search".

For p parameters, a minimum of N = p initial runs were required before the Δ criterion could be applied. This is a result of the least squares method which requires at least p normal equations for the estimation of p parameters. In this case p = 4, therefore, at least four initial runs were required to begin the iterative process.

From this point on, the iterative process should be followed using the Δ criterion to select the conditions for the next run. When the iterative process nears the "best" parameter estimates, $\hat{\theta}$, the Δ surfaces on

the grid tend to level out, making it difficult to distinguish a maximum (29). Also, in the vicinity of the best estimates the estimated values of the θ's are not changed significantly with each succeeding experiment. If the sole objective of the study were to estimate the parameters this would be the point to end the experiments. However, a second objective is to test the model, and data taken according to the Δ criterion may do this.

Data taken according to the Δ criterion often leads to data points which are clustered in groups within the region defined by the independent variables (11, 29). If this happens, the model may not be tested adequately over the entire range of independent variables. Additional runs should be conducted using settings of the independent variables in areas where data have not previously been taken, simply to test the model. For example, suppose the Δ criterion led to data which were taken only at high temperatures. Then, it would be desirable to conduct some runs at low temperatures to test the model. In addition, some replicate runs should be conducted for estimation of the experimental error.

IV. EQUIPMENT AND PROCEDURE

The three step iterative cycle of (1) design, (2) experiment, (3) analysis was used as the overall approach for obtaining the experimental data. A general description of the equipment and operating procedure of the experimental step is given in the following paragraphs. For the step by step operating procedure see Appendix F. The equipment-flow diagram is shown in Figure 1.

The experimental equipment used in this work consisted of the $NbOCl_3$ sublimer, the tubular reactor, and $NbCl_5$-$NbOCl_3$ condenser. The entire apparatus was made of pyrex. Argon at a constant and carefully measured rate entered the sublimer and became saturated with $NbOCl_3$. The saturated mixture passed through the heated connector tube to the plug flow reactor where $COCl_2$ entered and reacted with the $NbOCl_3$ to form $NbCl_5$ and CO_2. The $NbCl_5$ and unreacted $NbOCl_3$ were removed in the condenser. The CO_2, unreacted $COCl_2$, and argon passed on to a gas sampling tee where samples were removed through a rubber septum with a syringe and injected into the chromatograph.

The flow rate of 99.9 mole % $COCl_2$ to the reactor was controlled within the range 0.1-0.4 cc/sec STP by a monel valve. For all experiments except 16 and 17 a Matheson 600 tube rotameter with a pyrex ball float was used to monitor the $COCl_2$ flow rate. A Thermo-Systems model 1353 - AG mass flow meter was used for Experiments 16 and 17. This flow meter was damaged after Experiment 17 and replaced by the rotameter.

The $COCl_2$ flow meters were not calibrated because no satisfactory calibration method was found for either the mass flow meter or the rotameter. The $COCl_2$ flow meters were used simply to see if the $COCl_2$ rate remained

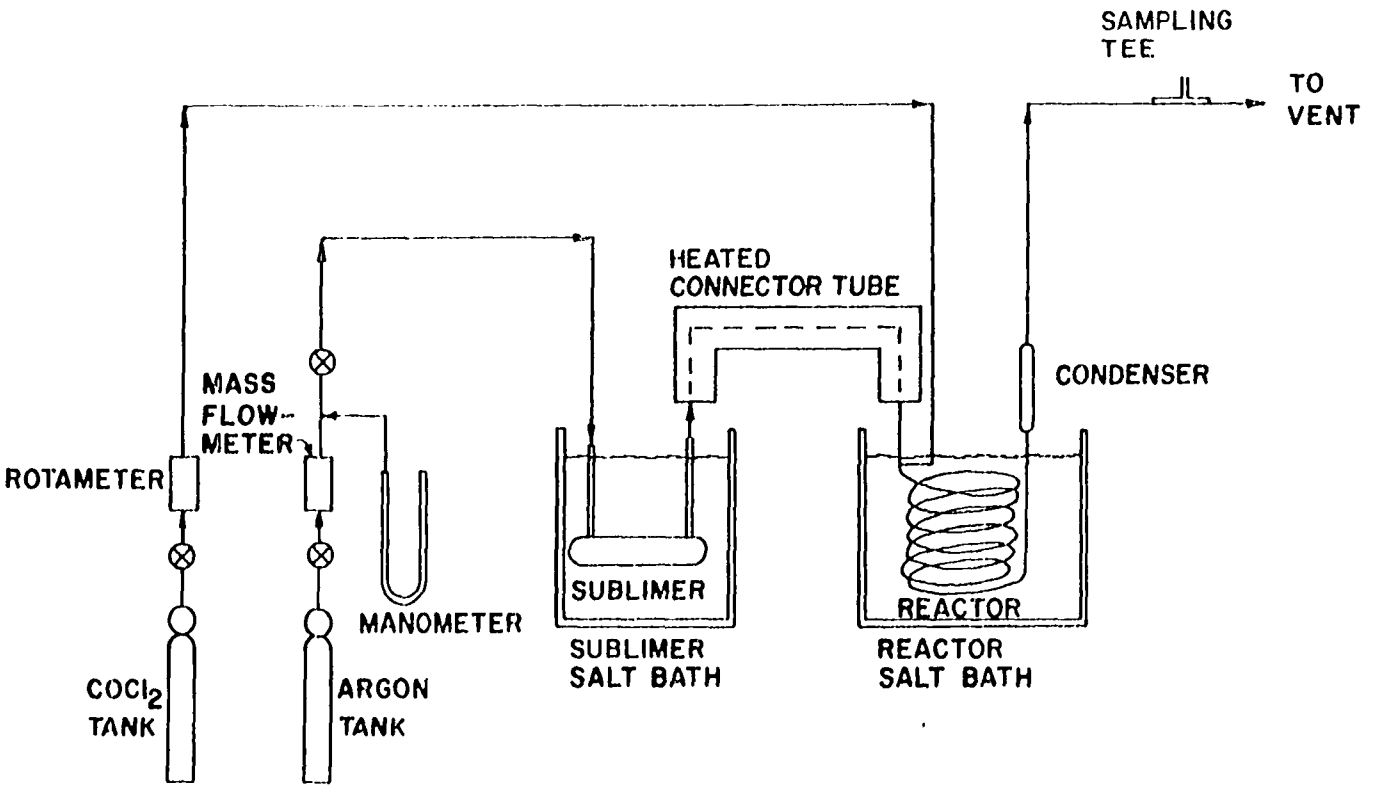

Figure 1. Equipment flow diagram

constant during a run.

The flow rate of 99.995 mole % argon was controlled in the range 0.1-0.4 cc/sec STP by a stainless steel micro-valve and measured by a Thermo-System Model 1351 mass flow meter. The flow meter was calibrated immediately before or after each experiment to minimize errors which resulted primarily from ambient temperature variations. The accuracy of the flow meter was reported to be ± 1.5% for temperature fluctuations of less than ± 2°C.

The system pressure was measured by a manometer filled with glycerine. Plugs in the lines or condenser were indicated by increases in the system pressure.

The 100 cc sublimer was filled with 5-8 grams of $NbOCl_3$, prepared by the method of Boesiger (6). The sublimer and reactor were emersed in molten nitrate salt maintained within the limits ± 0.2°C within the ranges 270-460°C. The salt bath temperatures were measured by calibrated platinum-13% rhodium thermocouples.

The two reactors were helical glass coils of 0.6 cm pyrex glass tubing. The nominal volumes were 72 cc and 340 cc. The actual volumes varied somewhat from the stated figures because the reactors were occasionally broken and had to be replaced or repaired.

The air cooled condenser was a 40 cc glass jacketed tube. The condenser was attached to the reactor and to the outlet line by pyrex ground glass joints held in place by steel clamps. When $NbOCl_3$ plugged a condenser, the condenser was easily removed by releasing the clamps and a clean condenser was clamped in place.

A 2.5 cc syringe was used to obtain samples at a sampling tee in the

vent line. The sample was removed through a rubber septum and injected into the chromatograph. The details on the operation of the chromatograph are in Appendix G.

The general experimental procedure was as follows. Calibration curves for the chromatograph and a flow calibration curve for the argon flowmeter were prepared shortly before or after each run. Before the run the salt baths were heated to operating temperatures, the silica gel of the chromatograph column was dryed thoroughly, and the reactor and lines were purged with argon.

The sublimer, loaded with $NbOCl_3$, was placed in the salt bath and connected to the argon line and heated connector tube. After one to two hours, the argon and $COCl_2$ rates were set to their run levels and the argon purge stream was stopped.

Salt bath temperatures, flow rate readings, pressure drop, and clock time were recorded every five minutes. The helium carrier gas rate for the chromatograph and the ambient temperature were recorded every 15-20 minutes. Other information recorded was the ambient pressure, the heater controller settings, and the bridge current, detector temperature, and column temperature of the chromatograph.

After the system had been at steady state for a sufficient time (See Appendix E), a sample was withdrawn from the sampling tee and injected into the chromatograph. The data for each run consisted of the analysis of the chromatograph sample plus the temperature and flow rate data.

Generally one or two more runs were conducted by resetting the flow rates. The sublimer and reactor temperatures were not changed. For each

experiment only two or three runs could be conducted because leaks developed at the joint between the reactor and condenser. The leaks were caused by build-up of deposits of Nb_2O_5 at the joint when the condensers were replaced.

V. METHOD OF CALCULATION

Five independent variables and one dependent variable from Equations 5 and 6 were calculated from the data of each run. These variables are:

Independent variables

C_{Total} = Molar density, g moles/liter

T = Reactor temperature, (°C)

C_{Ao} = Initial $NbOCl_3$ concentration, g moles/liter

C_{Bo} = Initial $COCl_2$ concentration, g moles/liter

τ = Space time, (seconds)

Dependent variable

y = g moles CO_2/g moles $COCl_2$, Ar, CO_2

Other possible variables such as flow rate, reactor volume, etc., can be be shown to be functions of these five or vice versa. Pressure could be an independent variable but in this study the pressure was essentially constant at atmospheric pressure.

C_{Total} was calculated from the ideal gas law using the reactor pressure, P_R, and the reactor temperature, T. T was assumed to be the temperature of the large salt bath. P_R was assumed to be the ambient pressure plus the system pressure corrected for the pressure drop up stream from the reactor.

C_{Ao} was not measured directly but instead was estimated using the vapor pressure equations of Gloor (20). The total $NbOCl_3$ and $NbCl_5$ equilibrium pressure, P_{NbT}; the $NbCl_5$ pressure, P_{NbCl_5}; and the $NbOCl_3$ pressure, P_{NbOCl_3}, were calculated by:

$$\log_{10} P_{NbT} = 13.533 - 6433/T_S$$

$$\log_{10} P_{NbCl_5} = 8.779 - 4680/T_S$$

$$P_{NbOCl_3} = P_{NbT} - P_{NbCl_5}$$

where T_S was the sublimer salt bath temperature in °K. The total pressure in the sublimer, P_S, was taken to be equal to the reactor pressure, P_R.

The flow rates of $NbOCl_3$ and $NbCl_5$ into the reactor were estimated from the argon flow rate through the sublimer and the pressures P_{NbCl_5}, P_{NbOCl_3}, and P_S. Finally, C_{Ao} was estimated by multiplying C_{Total} by the ratio of the $NbOCl_3$ flow rate to the total flow rate of gases in the reactor.

Originally, the $NbOCl_3$ rate was to be measured after each run by weighing the amount of $NbOCl_3$ collected in previously weighed condensers for a measured period of time. This method proved to be time consuming as well as questionable in accuracy (i.e. not all of the $NbOCl_3$ would collect in the condenser, particles would fall from the condenser when the condenser was removed, etc.). A number of runs were made, however, and as Table 1 shows, the measured results are within 5% of the flow rates predicted from Gloor's vapor pressure data. Therefore, Gloor's (20) vapor pressure equations were used to estimate the $NbOCl_3$ concentration. Although other vapor pressure equations are available on the $NbOCl_3$-Nb_2O_5-$NbCl_5$ system (36, 42, 43), Gloor's are probably the most reliable (See Appendix A).

C_{Bo} was calculated by multiplying C_{Total} by the ratio of the $COCl_2$ flow rate to the total flow rate. The $COCl_2$ flow rate was calculated by multiplying the argon flow rate times the ratio of the volume of CO_2 and $COCl_2$ in the sample to the volume of argon in the sample.

The space time, τ, was calculated by dividing the reactor volume (cc) by the total flow rate (cc/sec) through the reactor at T and P_R. The reactor volume was corrected for the expansion of pyrex glass.

Table 1. Comparison of measured flow rate of $NbOCl_3$ and $NbCl_5$ with flow rate estimated from vapor pressure data*

Run Number	Sublimer Temperature (°C)	Gas Rate (cc/sec)	Ave Measured Flow Rate (gm $NbOCl_3$/hr)	Ave Estimated* Flow Rate (gm $NbOCl_3$/hr)	% Differ.
1-17	276.0	0.204	0.629	0.606	-3.7
1-21	275.5	0.201	0.591	0.579	-2.0
1-24	275.5	0.310	0.901	0.895	-0.7
1-27	276.0	0.307	0.959	0.913	-4.8
1-30	277.25	0.303	0.940	0.956	+1.7
1-35	300.0	0.196	2.144	2.258	+5.4

*Estimated from Gloor's (20) vapor pressure equations

The dependent variable, y, is simply the volume of CO_2 in the sample divided by total sample volume. The sample volume was the volume of the syringe corrected to standard conditions minus a small correction for air leakage into the syringe.

An average volume of the air leakage was obtained by injecting a number of CO_2 samples into the chromatograph and measuring the air volume in each sample. The air leakage was small, ranging from 0.003 cc STP to 0.012 cc STP. A typical average volume for the air leakage was 0.0077 cc.

In some of the experiments a correction was necessary for a small amount of $COCl_2$ decomposition, (less than 1.0% of the sample). This decomposition was too large to be explained by thermal decomposition. Since no exact method for accounting for this $COCl_2$ decomposition was known, an approximate correction was made by assuming that the CO concentration was equal to the Cl_2 concentration and that CO and Cl_2 were present throughout the reactor at their average concentrations.

VI. RESULTS

Experimental data were taken essentially as described in III. Theory and are summarized in Table 2. These data were used for parameter estimation and model discrimination. In addition, the data were used to evaluate and study some aspects of the Δ criterion experimental design.

A. Parameter Estimation and Model Discrimination

The parameters of Models 1-3 described earlier were estimated by nonlinear least squares from the data of Table 2. Table 3 shows these models listed according to their "goodness of fit", i.e., low sum of squares of residuals, low standard deviation of the residuals, etc. The final parameter estimates for the models are also given in Table 3.

In addition to Model 3, four other rate equations involving transistion intermediates were considered. These four models fit the data almost as well as Model 2 but were rejected for the following reasons. Three of these models had excessively high parameter estimates that caused the rate equations to degenerate to the form of Model 2. The fourth was rejected because of a physically unrealistic negative rate constant.

Other special cases of Model 1 were tested by fixing θ_3 and θ_4 at various combinations of 0.5, 1.0 and 1.5 and obtaining the best values of A and E by nonlinear least squares. For these models the sums of squares of the residuals were from three to ten times higher than for Model 1 and the F test ratios were also from three to ten times as high.

The values of $\hat{y}$ were estimated from the data of Table 2 using Model 1 with the final parameter estimates ($A = 1.461 \times 10^6$, $E = 23316$, $\theta_3 = 0.829$, $\theta_4 = 0.921$). The values of y, $\hat{y}$ and the residuals are given in Table 4 and $\hat{y}$ vs. y are shown in Figure 2. For comparison, values of $\hat{y}$ were also cal-

Table 2. Experimental data

Run Number	$NbOCl_3$ [a] Concentration (g moles/liter)	$COCl_2$ [a] Concentration (g moles/liter)	Reactor Temperature (°C)	Space [b] Time (sec)	Molar [a] Density (g moles/liter)	Moles CO_2 / Moles Ar,$COCl_2$,CO_2
9.1*	0.000450	0.0105	452.8	90.9	0.0164	0.0177
9.2*	0.000450	0.0110	452.7	84.6	0.0165	0.0172
9.3*	0.000473	0.0106	451.5	88.9	0.0164	0.0157
10.1	0.000507	0.0116	357.3	488.7	0.0187	0.0082
10.2*	0.000457	0.0121	357.3	454.4	0.0187	0.0070
10.3*	0.000452	0.0123	356.6	439.2	0.0187	0.0065
10.4*	0.000453	0.0122	357.0	447.1	0.0186	0.0071
10.5*	0.000426	0.0122	356.2	451.6	0.0187	0.0062
11.4*	0.001215	0.0123	346.2	487.8	0.0192	0.0153
11.5*	0.001256	0.0122	346.5	467.6	0.0192	0.0129
12.1	0.001145	0.0094	456.7	95.4	0.0163	0.0354
12.2*	0.001085	0.0100	457.0	87.1	0.0162	0.0342
12.3*	0.001066	0.0101	456.6	82.7	0.0162	0.0323
12.4*	0.001111	0.0099	457.1	87.0	0.0163	0.0337
13.1*	0.001364	0.0110	347.2	516.4	0.0190	0.0161
13.2*	0.001254	0.0117	348.0	488.0	0.0189	0.0149
13.3*	0.001396	0.0110	347.5	534.5	0.0189	0.0163
13.4	0.001575	0.0104	346.9	542.3	0.0189	0.0164
16.2	0.001615	0.0067	448.4	98.8	0.0163	0.0379
16.3	0.001733	0.0066	449.6	84.8	0.0162	0.0360
17.3	0.002753	0.0044	447.0	69.6	0.0163	0.0327
18.1	0.003186	0.0073	352.9	436.9	0.0189	0.0263
19.1	0.003227	0.0078	338.4	406.3	0.0192	0.0200
19.2	0.003469	0.0067	338.7	447.9	0.0192	0.0197

[a] Concentrations evaluated at reactor temperature and pressure
[b] Space times less than 100 seconds obtained with 72 cc reactor
* Replicate runs

Table 2 (Continued)

Run Number	$NbOCl_3$ [a] Concentration (g moles/liter)	$COCl_2$ [a] Concentration (g moles/liter)	Reactor Temperature (°C)	Space [b] Time (sec)	Molar [a] Density (g moles/liter)	Moles CO_2 / Moles Ar,$COCl_2$,CP_2
21.1*	0.001928	0.0090	449.5	58.3	0.0164	0.0342
21.2*	0.001911	0.0091	449.3	58.5	0.0164	0.0331
21.3*	0.001853	0.0094	449.9	56.9	0.0164	0.0306
22.1	0.001208	0.0118	347.0	473.9	0.0190	0.0115
22.2	0.001080	0.0127	346.1	421.7	0.0190	0.0095
23.1*	0.001928	0.0085	449.7	68.0	0.0162	0.0348
23.2*	0.001947	0.0086	449.5	66.5	0.0162	0.0360
24.1*	0.002693	0.0058	339.6	444.0	0.0192	0.0112
24.2*	0.002654	0.0060	340.5	431.6	0.0191	0.0111
25.1*	0.002572	0.0050	429.6	382.4	0.0168	0.0829
25.2*	0.002551	0.0050	429.7	369.6	0.0168	0.0781
28.1*	0.002542	0.0079	389.6	394.6	0.0177	0.0653
28.2*	0.002588	0.0079	398.3	394.3	0.0177	0.0674
29.1*	0.002635	0.0068	408.1	461.0	0.0174	0.0770
29.2*	0.002725	0.0065	408.0	469.2	0.0173	0.0780

Table 3. Comparison of kinetic models

Model No.	Rate Equation [a]	Sum of Squares of Residuals x 10^3	Standard Error of y	$F = \frac{s'^2}{s_e^2}$	$A^b \times 10^{-6}$	E (cal/ g mole)	Θ_3 or $A' \times 10^{-6}$	Θ_4 or E' (cal/g mole)
1	$r=kC_A^{\Theta_3}C_B^{\Theta_4}$	0.1538	0.00210	7.39	1.461 (±50.8%)	23316 (±1.7%)	Θ_3=0.829 (±5.5%)	Θ_4=0.921 (±5.9%)
3	$r=\frac{-kC_AC_B}{k'C_A+1.0}$	0.1737	0.0023	8.47	20.32 (±6.1%)	24650 (±4.2%)	A'=0.079 (±42.6%)	E'=9069 (±85.9%)
2	$r=kC_AC_B$	0.2105	0.0039	10.46	10.21 (±1.7%)	23946 (±1.7%)	--	--

[a] $k = A \exp(-E/RT)$

$k' = A' \exp(-E/RT)$

[b] Dimensions of A and A' consistent with concentrations in g moles/liter and time in sec.

Table 4. Residuals, $\hat{y}$ and y for Model 1 with best parameter estimates

Run Number	y [a]	$\hat{y}$ [b]	Residuals
9.1	0.01769	0.01483	0.00287
9.2	0.01724	0.01439	0.00285
9.3	0.01568	0.01509	0.00059
10.2	0.00699	0.00754	-0.00055
10.3	0.00651	0.00720	-0.00069
10.4	0.00709	0.00739	-0.00029
10.5	0.00621	0.00691	-0.00070
11.4	0.01534	0.01402	0.00132
11.5	0.01293	0.01392	-0.00099
12.2	0.03422	0.03365	0.00057
12.3	0.03227	0.03182	0.00045
12.4	0.03366	0.03405	-0.00038
13.1	0.01611	0.01559	0.00051
13.2	0.01489	0.01479	0.00010
13.3	0.01626	0.01644	-0.00018
21.1	0.03415	0.03338	0.00077
21.2	0.03310	0.03336	-0.00026
21.3	0.03065	0.03291	-0.00226
23.1	0.03478	0.03698	-0.00221
23.2	0.03596	0.03670	-0.00074
24.1	0.01120	0.01174	-0.00054
24.2	0.01112	0.01190	-0.00078
25.1	0.08290	0.08195	0.00095
25.2	0.07808	0.07973	-0.00165
28.1	0.06527	0.06339	0.00188
28.2	0.06742	0.06398	0.00344
29.1	0.07698	0.08045	-0.00346
29.2	0.07801	0.08130	-0.00329
10.1	0.00822	0.00850	-0.00028
12.1	0.03541	0.03579	-0.00038
13.4	0.01640	0.01766	-0.00126
16.2	0.03791	0.03406	0.00385
16.3	0.03598	0.03256	0.00341
17.3	0.03273	0.02870	0.00403
18.1	0.02632	0.02480	0.00152
19.1	0.02002	0.01611	0.00392
19.2	0.01965	0.01679	0.00286
22.1	0.01155	0.01357	-0.00202
22.2	0.00954	0.01145	-0.00191

[a] Measured ratio of moles of CO_2 to moles CO_2, Ar and $COCl_2$

[b] Calculated ratio of moles CO_2 to moles CO_2, Ar and $COCl_2$

Figure 2. The $\hat{y}$ vs. y values for Model 1 and final parameter estimates ($A = 1.461 \times 10^6$, $E = 23316$, $\theta_3 = 0.829$, $\theta_4 = 0.921$) with $\pm$ 2s lines (— — —) where s = 0.0021

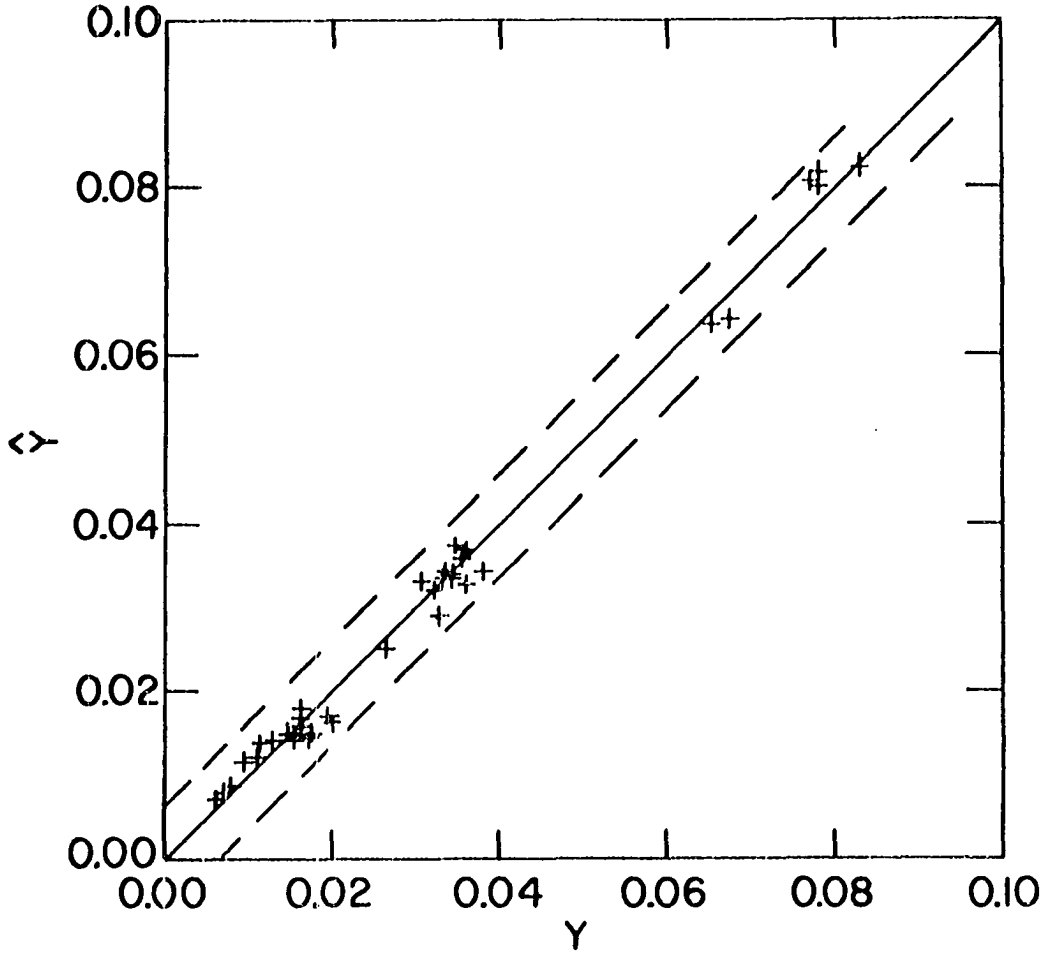
0.10
0.08
0.06
0.04
0.02
0.00
<Y>
0.00
0.02
0.04
0.06
0.08
0.10
Y

culated using Model 1 with Boesiger's (7) parameter estimates (A = 0.526 x 10^6, E = 21209, Θ_3 = 0.917, Θ_4 = 1.013) and Boesiger's data. These $\hat{y}$ vs. y values are shown in Figure 3 with the $\hat{y}$ vs. y values of this work. The ± 2s lines for Boesiger's data (s = 0.031) and ± 2s lines for this work (s = 0.0021) are also in Figure 3, where s is the standard error (standard deviation) of y. It is apparent from Figure 3 that Boesiger's data covered a greater range of y values and were much more scattered than the data of this work.

Figure 4 is a $\hat{y}$ vs. y plot of $\hat{y}$ values calculated using the final parameters of this work and Boesiger's data and $\hat{y}$ values calculated using Boesiger's parameters and the data of Table 2. Figure 4 shows that the parameters of this work predict high values of $\hat{y}$ from Boesiger's data, but the $\hat{y}$'s generally lie within the ± 2s line (s = 0.031). Boesiger's parameters predict low $\hat{y}$'s from the data of Table 2, and the $\hat{y}$'s lie outside the ± 2s line (s = 0.0021) of this work.

Figure 5 shows a number of plots of the residuals vs. such variables as y; run number; initial $NbOCl_3$ concentration, C_{Ao}; initial $COCl_2$ concentration, C_{Bo}; reactor temperature, T; and space time, τ. It appears from the plots that there is no correlation between the residuals and these variables.

A four dimensional confidence region of the parameters is "difficult" to represent graphically. However, two dimensional plots of $S(\theta)$ as a function of two parameters were made, holding the other two constant at the minimum sum squares estimates. An approximate 95% confidence region for Θ_3 and Θ_4 with A = 1.461 x 10^6 and E = 23316 is illustrated in Figure 6. Also, an approximate 95% confidence region for A and E with Θ_3 = 0.829 and Θ_4 = 0.921 is represented in Figure 7.

The boundary of the confidence region was calculated by:

Figure 3. The $\hat{y}$ vs. y values for Model 1 showing Boesiger's results (o) and the results of this work (+)

± 2s line for this work (s = 0.0021) - - - -

± 2s line for Boesiger's results (s = 0.031) —— —— ——

Note scale change for $\hat{y}$ and y values less than 0.1

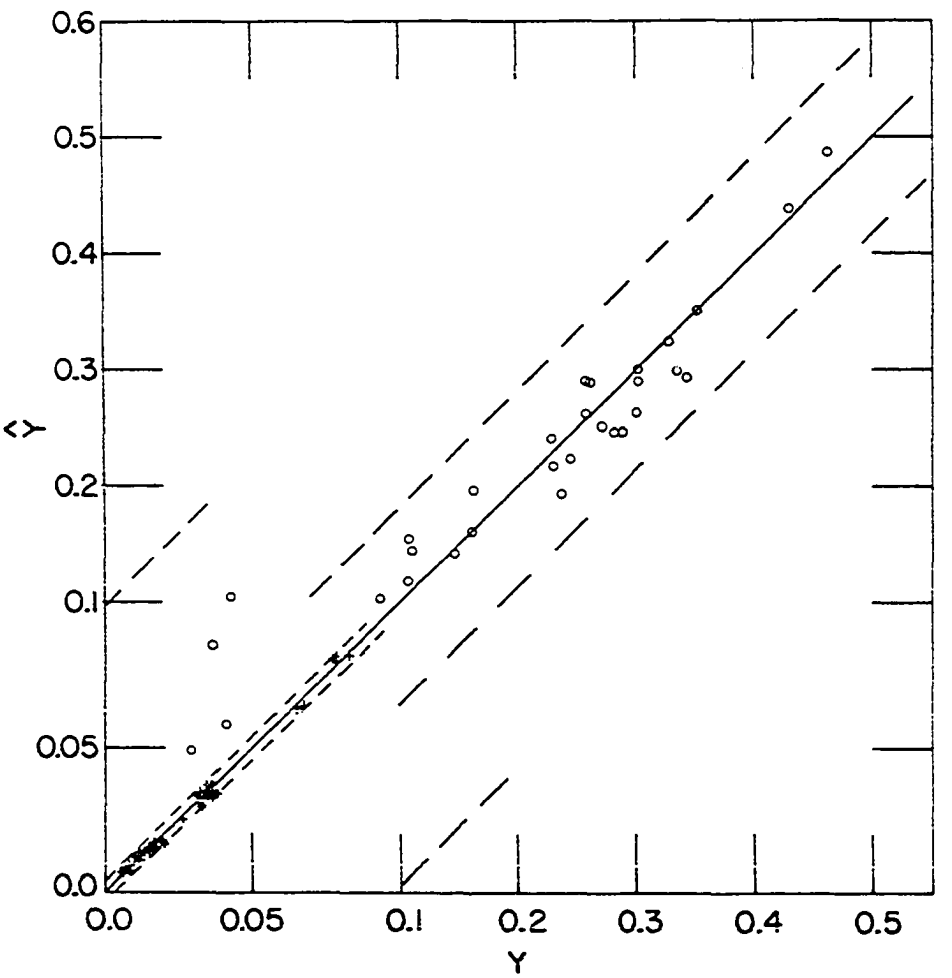
0.6
0.5
0.4
0.3
0.2
0.1
0.05
0.0
<Y
0.0
0.05
0.1
0.2
0.3
0.4
0.5
Y

Figure 4. The $\hat{y}$ vs. y values for Model 1 using Boesiger's data with the parameters of this work (+) and the data of Table 2 with Boesiger's parameters (o)

$\pm$ 2s lines for this work (s = 0.0021) - - - -

$\pm$ 2s lines for Boesiger's results (s = 0.031) —— —— .

Note change of scale for $\hat{y}$ and y values less than 0.1

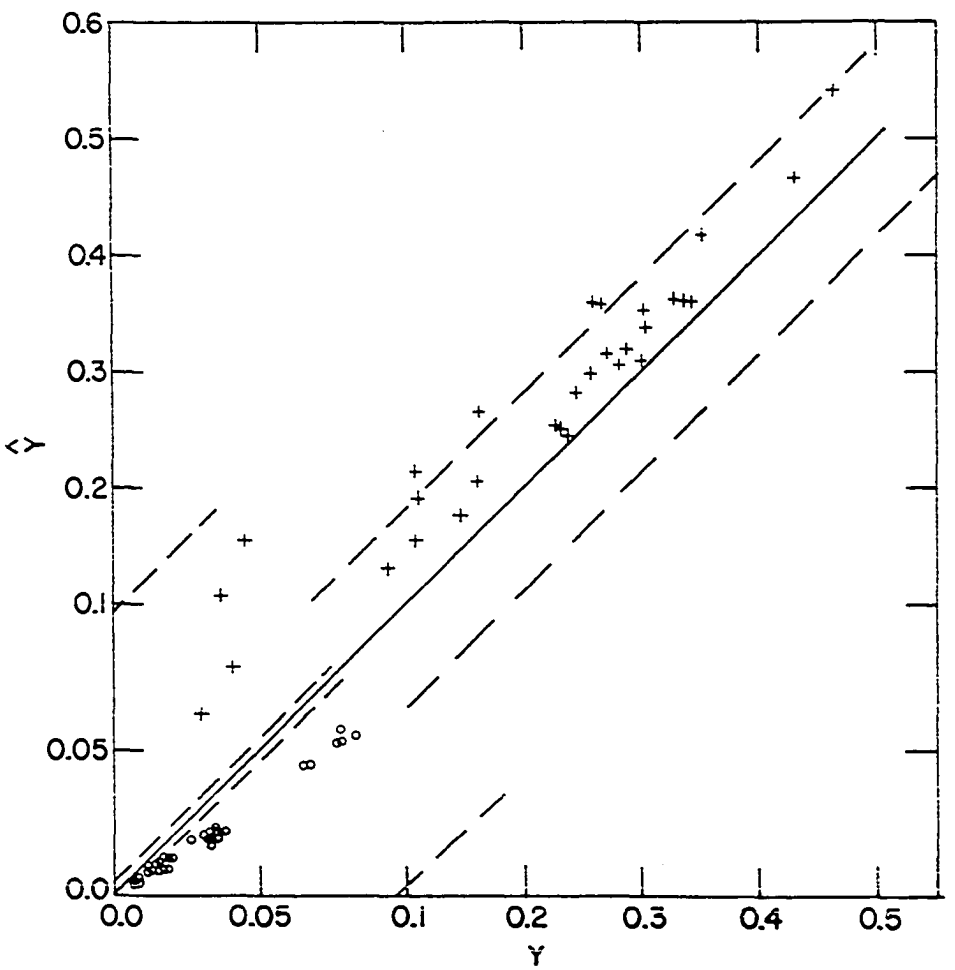
0.6
0.5
0.4
0.3
0.2
0.1
0.05
0.0
<Y
0.0
0.05
0.1
0.2
0.3
0.4
0.5
Y

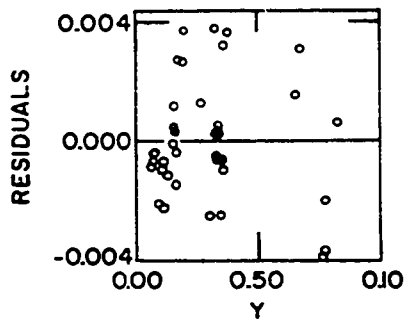

5(a)

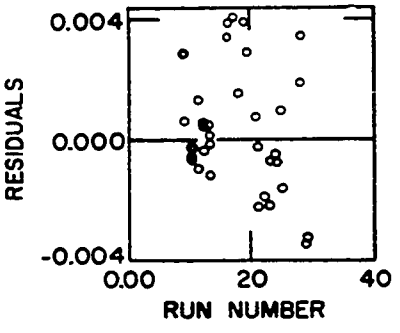

5(b)

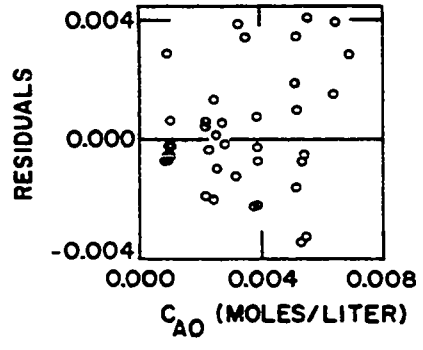

5(c)

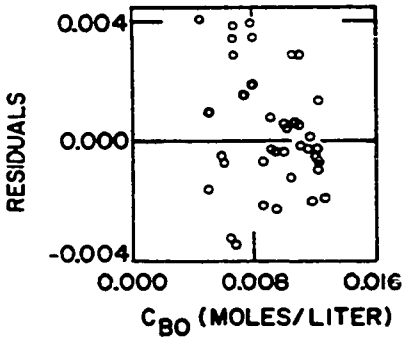

5(d)

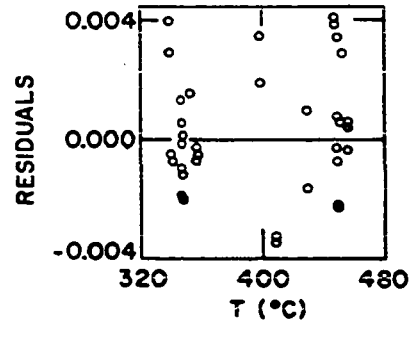

5(e)

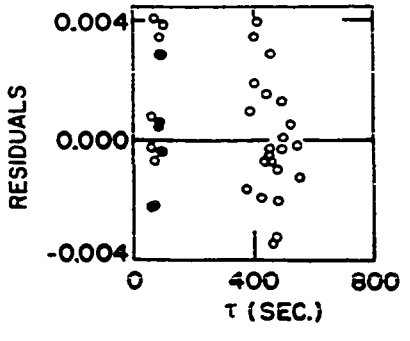

5(f)

Figure 5. Residuals $(y - \hat{y})$ vs. y, run number, C_{Ao}, C_{Bo}, T and τ

Figure 6. Approximate 95% confidence regions for θ_3 and θ_4 at fixed values of E (cal/g mole) and A*

*Dimensions consistent with concentrations in g moles/liter and time in seconds

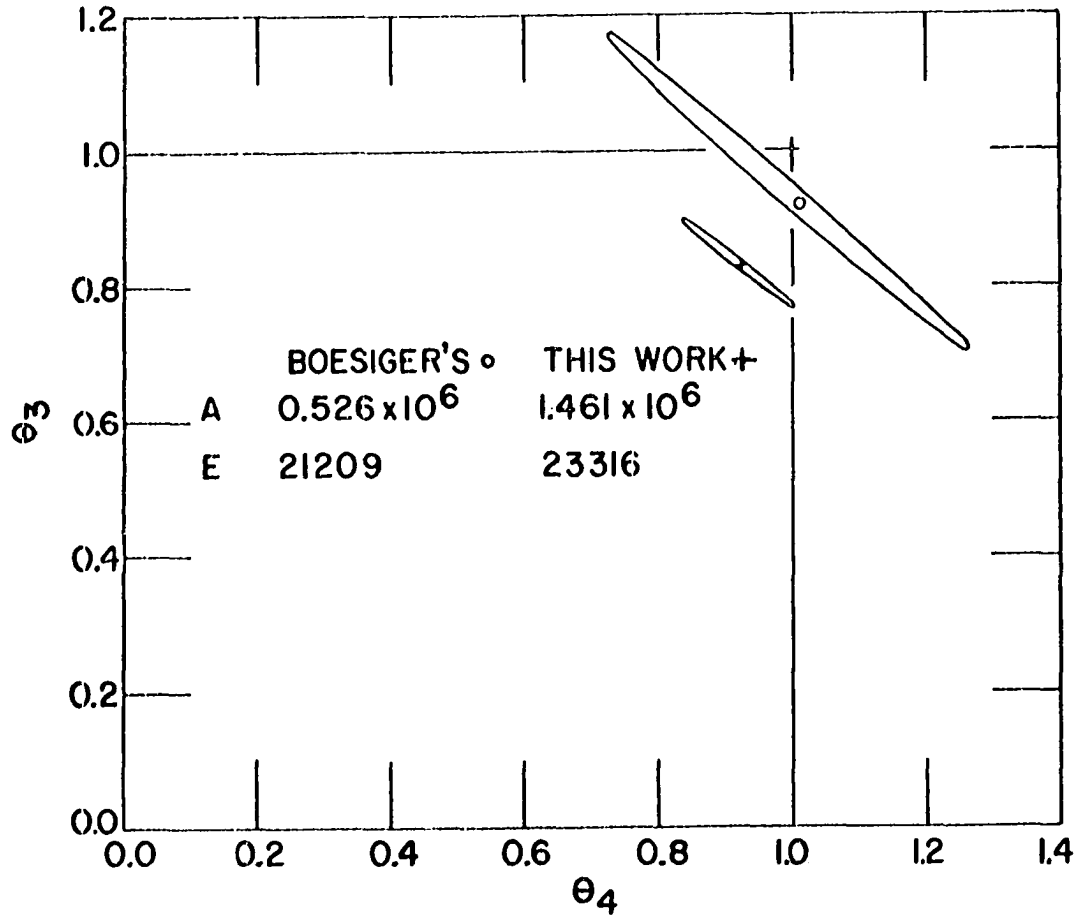
1.2
1.0
0.8
0.6
0.4
0.2
0.0
0.0
0.2
0.4
0.6
0.8
1.0
1.2
1.4
Θ_3
Θ_4
BOESIGER'S o
THIS WORK+
A
0.526 x 10^6
1.461 x 10^6
E
21209
23316

Figure 7. Approximate 95% confidence regions for E (cal/g mole) and A* at fixed values of θ_3 and θ_4

---

*Dimensions consistent with concentrations in g moles/liter and time in seconds

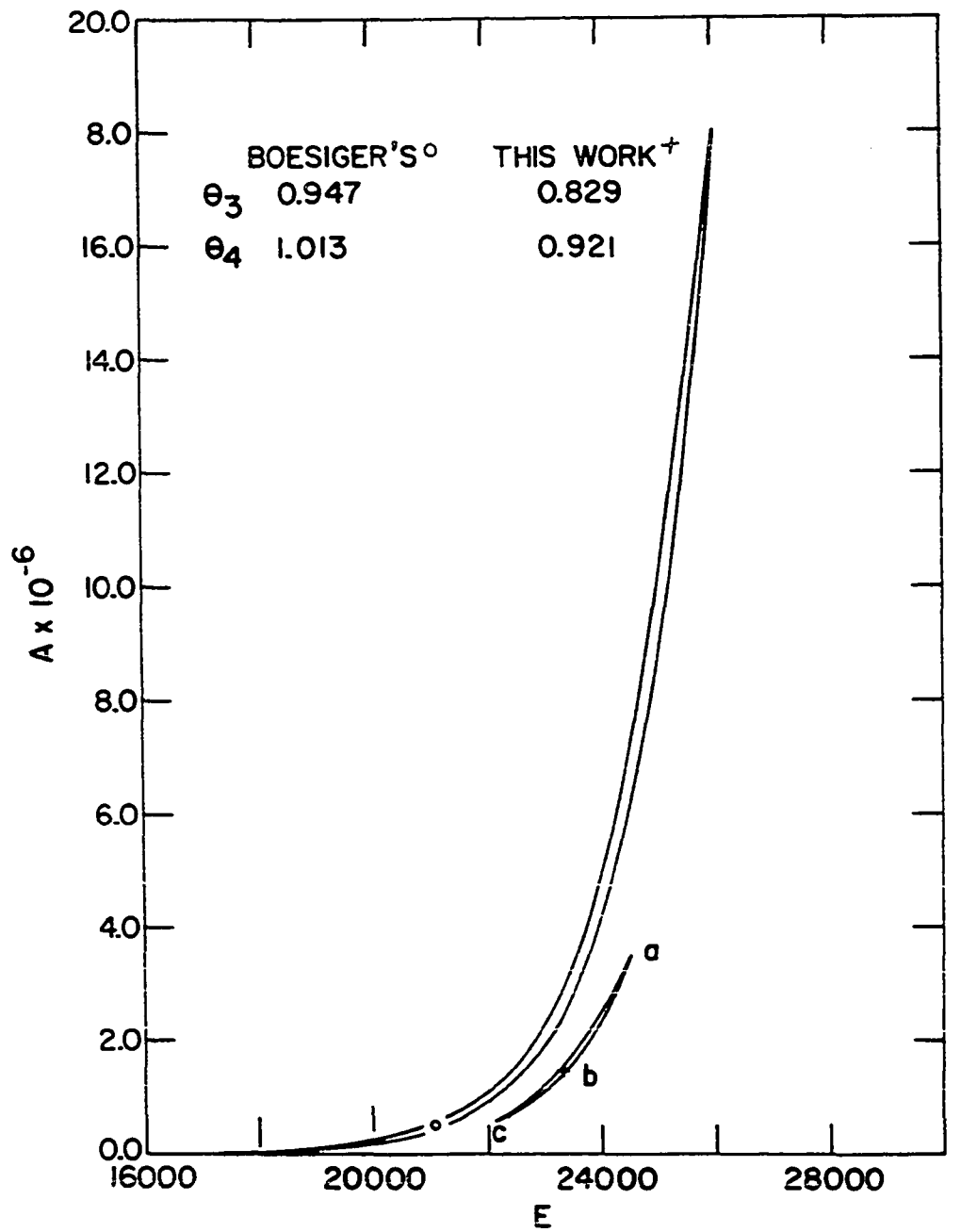
20.0
8.0
16.0
14.0
12.0
10.0
8.0
6.0
4.0
2.0
0.0
A x 10^-6
BOESIGER'S°
THIS WORK+
θ3 0.947
0.829
θ4 1.013
0.921
a
b
c
16000
20000
24000
28000
E

$$S(\theta) = S(\hat{\theta})[1 + \frac{p}{N-p} F(p, N-p, 0.95)]$$

where the minimum sum of squares, $S(\theta)$, for Model 1 was 1.538×10^{-4}; the number of parameters, p, was 4; the number of runs, N, was 39; and the F distribution with 4 and 35 degrees of freedom, $F(p, N-p, 0.95)$ was 2.65. When these numbers were placed in the equation, $S(\theta) = 2.00 \times 10^{-4}$.

In the same way, approximate 95% confidence regions for Boesiger's data and parameter estimates are shown in Figures 6 and 7. For Boesiger's data, $S(\hat{\theta}) = 0.0249$, $p = 4$, $N = 30$, $F(4, 26, 0.95) = 2.74$ and $S(\theta) = 0.0354$. It is apparent the confidence regions for this study are much smaller. The contours for all of the confidence regions are attenuated and the parameters are highly correlated.

Since A and E are highly correlated, any combination of A and E within the 95% confidence region yield values of the rate constant, k, that differ by less than 10% in the range 350-450°C. In Figure 8, k values were plotted vs. the reciprocal of the temperature, °K, for points a ($A = 3.41 \times 10^6$, $E = 24465$); b ($A = 1.461 \times 10^6$, $E = 23316$); and c ($A = 0.6 \times 10^6$, $E = 22120$) of Figure 7. The k values are nearly equal at the intermediate temperatures and diverge at the high and low temperatures. Apparently, more precise estimates of A and E could be obtained only by taking data over a greater temperature range.

B. Application of the Δ Criterion

To clarify the discussion in the following sections, the terms "experiment number" and "run number" must be explained. The "experiment number" refers to one of the 29 experiments numbered in the order in which they were conducted. Each experiment consisted of several runs that were replications or near replications. A "run number" such as 9.2 of Table 2 refers to the

Figure 8. Rate constant, k, vs. reciprocal of reactor temperature, T (°K), for values of E (cal/g mole) and A* at points a, b and c of 95% confidence region of Figure 7

---

*Dimensions consistent with concentrations in g moles/liter and time in seconds

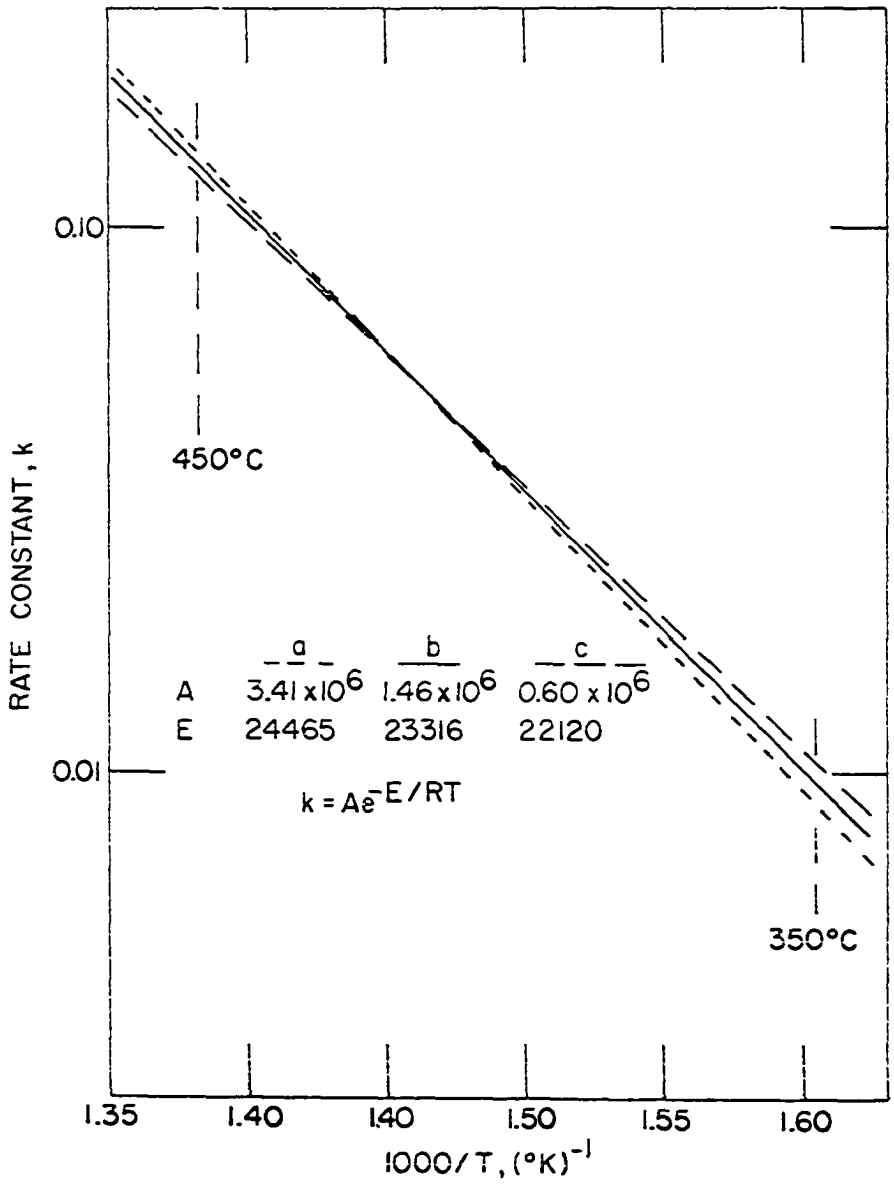
RATE CONSTANT, k
0.10
0.01
450°C
350°C
a
b
c
A
3.41 x 10^6
1.46 x 10^6
0.60 x 10^6
E
24465
23316
22120
k = Ae^-E/RT
1.35
1.40
1.40
1.50
1.55
1.60
1000/T, (°K)^-1

second run of Experiment 9.

The experimental design called for a minimum of four experiments to provide initial parameter estimates. To accomplish this goal Experiments 9-12 were conducted at various combinations of high and low settings of the temperature , $NbOCl_3$ concentrations, and space times. The $COCl_2$ concentration and total concentration varied less than 20% between experiments. In addition, Experiment 13 was conducted in an attempt to replicate Experiment 11. The initial parameter estimates after Experiment 13 were: $A = 16.6 \times 10^6$, $E = 24143$, $\theta_3 = 0.784$, $\theta_4 = 1.388$.

The independent variables for the experiments following Experiment 13 should have been chosen by the Δ criterion. Unfortunately, an error was made in the Δ criterion computer program, and this error was not discovered until Experiment 24.

As a result, the conditions for Experiment 25 were the first to be chosen using the Δ criterion. The conditions for Experiments 28 and 29 were also chosen by the Δ criterion. The parameter estimations at each stage of this experimental design are shown in Table 5. The figures in parenthesis next to the parameter estimates are the estimated standard errors of the parameters.

If the correct Δ criterion computer program had been available after Experiment 13, fewer experiments would have been required to estimate the parameters. To illustrate this without conducting more experiments the following strategy was used.

Initial parameter estimates were obtained using the data of Experiments 9-13. This information was used to choose the settings of the next experiment by the Δ criterion. However, the choice of the independent variable

Table 5. Sequential experimental design for Model 1 - 13 initial experiments

Experiment Numbers	$A^* \times 10^{-6}$	E (cal/g mole)	θ_3	θ_4
9-13, 16-19, 21-24	0.141 (± 52.1%)	22874 (± 2.1%)	0.744 (± 4.9%)	0.613 (± 11.2%)
9-13, 16-19, 21-25	1.119 (± 48.4%)	23233 (± 1.6%)	0.822 (± 5.3%)	0.887 (± 5.6%)
9-13, 16-19, 21-25, 28	1.362 (± 45.2%)	23178 (± 1.6%)	0.843 (± 4.9%)	0.906 (± 5.3%)
9-13, 16-19, 21-25, 28, 29	1.461 (± 50.4%)	23316 (± 1.7%)	0.829 (± 5.5%)	0.921 (± 5.9%)

*Dimensions of A consistent with concentration in g moles/liter and time in sec.

settings was restricted to those of the eleven experiments conducted after Experiment 13 (Experiments 16-19, 21-25, 28 and 29). Experiment 25 was chosen in this manner. New parameter estimates were obtained using the data of Experiments 9-13 and 25, and the Δ criterion was used to select Experiment 28 from the remaining ten experiments (16-19, 21-24, 28, 29). This sequential design was repeated for choosing Experiments 23, 18, and 19.

Table 6 shows the parameter estimates (A, E, θ_3 and θ_4) for Model 1 after each experiment of the experimental design sequence (25-28-23-18-19). The final estimates of the parameters from all 16 experiments is shown in the last row of Table 6 for reference.

Since the experimental design sequence of Table 6 was restricted to Experiments 16-19, 21-25, 28 and 29, the Δ 's chosen were not necessarily the largest possible within the range of the independent variables. To examine the Δ values at each step in the design sequence, grids were constructed for each of 41 combinations of $NbOCl_3$, $COCl_2$ and Ar flow rates within the limits of those variables. The "fine grid search" described in III. Theory was used.

Table 7 shows the maximum and minimum Δ's and the ratio of the maximum Δ to the minimum Δ at each stage of the design. In general, the relative range of the Δ values was reduced and the size of the Δ's was increased with each succeeding experiment. For instance, after Experiment 13 the ratio of Δ maximum to Δ minimum was 180, but by the final experiment the ratio was 1.34. The Δ's in the column at the right in Table 7 are the actual Δ values for the experiments chosen at each stage of the experimental design for the sequence of experiments of Table 6.

Table 6. Sequential experimental design for Model 1 - 5 initial experiments

Experiment Numbers	A* x 10^{-6}	E (cal/g mole)	θ_3	θ_4
9-13	16.588 (± 239.2%)	24143 (± 3.4%)	0.784 (± 8.1%)	1.388 (± 32.7%)
9-13, 25	0.524 (± 65.3%)	23293 (± 1.7%)	0.734 (± 7.2%)	0.887 (± 7.5%)
9-13, 25, 28	3.702 (± 50.9%)	23676 (± 2.0%)	0.869 (± 4.9%)	1.000 (± 5.4%)
9-13, 25, 28, 23	1.117 (± 43.5%)	23054 (± 1.7%)	0.818 (± 4.6%)	0.928 (± 5.0%)
9-13, 25, 28, 23, 18	1.169 (± 42.3%)	22997 (± 1.6%)	0.822 (± 4.5%)	0.930 (± 4.9%)
9-13, 25, 28, 23, 18, 19	1.105 (± 45.5%)	22754 (± 1.7%)	0.836 (± 4.8%)	0.936 (± 5.3%)
For all 16 experiments	1.461 (± 50.4%)	23316 (± 1.7%)	0.829 (± 5.5%)	0.921 (± 5.9%)

*Dimensions of A consistent with concentrations in g moles/liter and time in sec.

Table 7. Experimental design Δ values

Experiment Numbers	Maximum Δ $\times 10^{16}$	Minimum Δ $\times 10^{16}$	$\frac{\text{Maximum } \Delta}{\text{Minimum } \Delta}$	Chosen Δ $\times 10^{16}$	
9-13	0.036	0.00020	180	0.022	(Exp. 25)
9-13, 25	100	29	3.45	85	(Exp. 28)
9-13, 25,28	6.7	3.3	2.30	5.1	(Exp. 23)
9-13, 25, 28, 23	45	26	1.73	38	(Exp. 18)
9-13, 25, 28, 23, 18	57	34	1.67	45	(Exp. 19)
For all 16 experiments	195	145	1.34	---	

Grids of the type shown in Figure 9 were made after each experiment for the flow rates of $NbOCl_3$, $COCl_2$ and argon. These grids were used to scan the Δ surfaces to see if there were any unusual features. The "fine" grids were similar except the ordinate was in 10°C increments and the abcissa consisted of only two volumes (72 cc and 340 cc).

To illustrate some of the characteristics of the "coarse" grids, Figure 10 shows the Δ surfaces at three stages of the experimental design sequence of Table 6. The upper Δ surface was made using the data of the initial experiments (Experiments 9-13) for the flow rate settings of the first Δ criterion experiment (Experiment 25). The middle Δ surface was made using the data of Experiments 9-13 and 25 at the flow rate settings of the second Δ criterion experiment (Experiment 28), and the bottom Δ surface was made using the data of the Experiments 9-13, 25, 28, 23 and 18 for the flow rate settings of the final experiment of the sequence (Experiment 19).

The Δ surfaces of Figure 10 are typical of Δ surfaces at other settings of the flow rates at various stages of the experimental design. There are no peaks or depressions and the Δ surfaces appear to slope smoothly upward in the direction of the high temperature-high volume boundaries. Grids made at other stages had Δ surfaces that sloped in other directions and a few grids indicated that the Δ surfaces had small ridges.

Figure 10 illustrates clearly how the Δ surfaces flattened out after more Δ criterion experiments were conducted. In fact, the Δ surfaces of Fig Figure 10(c) for the final Δ criterion experiment (Experiment 19) is essentially a flat plane. This means that any combination of the settings of the

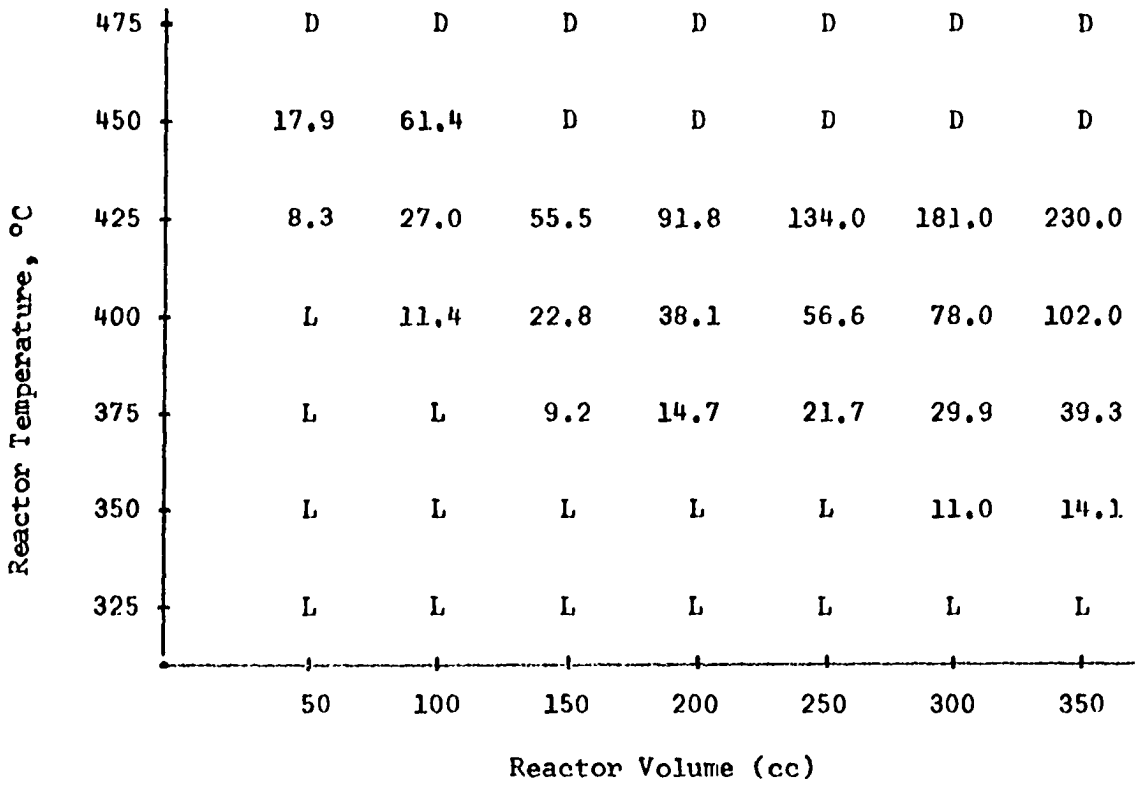

Note: The numbers in the grid are Δ values x 10^{20}

D represents $COCl_2$ decomposition too high (greater than 0.1 volume %)

L represents CO_2 concentration too low to be measured accurately (less than 0.8 volume %)

Flow rates of $NbOCl_3$, $COCl_2$, and argon were 0.0564, 0.109, 0.203 cc/sec, respectively.

Figure 9. Typical coarse grid for Δ using the data of Experiments 9-13 at flow rate conditions of Experiment 25

Figure 10. Surfaces of Δ grid at three stages of the experimental design of Table 6

10(a) Surfaces of Δ grid after Experiments 9-13 for flow rate conditions of Experiment 25 ($NbOCl_3$ flow rate = 0.056, $COCl_2$ flow rate = 0.109, Ar flow rate = 0.203)

10(b) Surfaces of Δ grid after Experiments 9-13 and 25 for flow rate conditions of Experiment 28 ($NbOCl_3$ flow rate = 0.056, $COCl_2$ flow rate = 0.174, Ar flow rate = 0.155)

10(c) Surfaces of Δ grid after Experiments 9-13, 25, 28, 23, and 18 for flow rate conditions for Experiment 19 ($NbOCl_3$ flow rate = 0.063, $COCl_2$ flow rate = 0.137, Ar flow rate = 0.163)

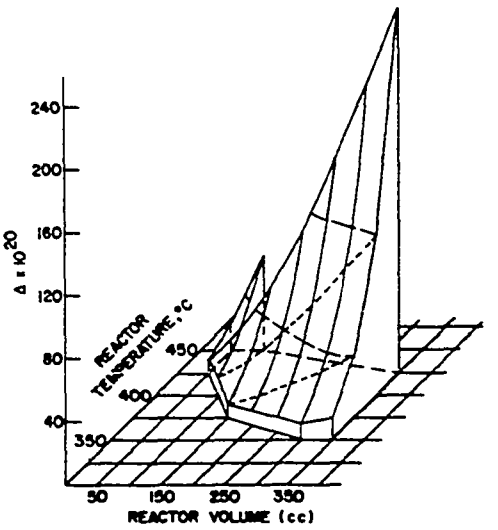
240
200
160
120
80
40
Δ x 10^20
REACTOR TEMPERATURE, °C
450
400
350
50
150
250
350
REACTOR VOLUME (cc)

(a)

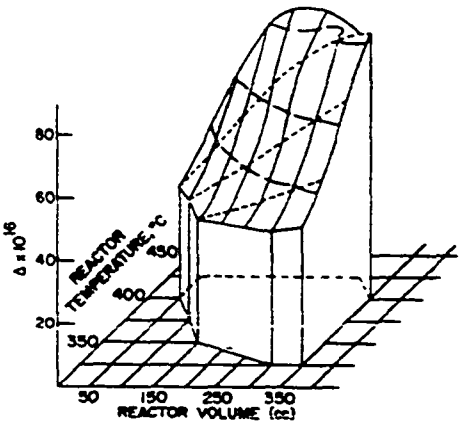
80
60
40
20
Δ x 10^16
REACTOR TEMPERATURE, °C
450
400
350
50
150
250
350
REACTOR VOLUME (cc)

(b)

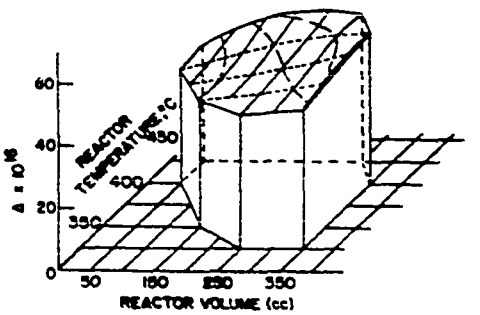
60
40
20
0
Δ x 10^16
REACTOR TEMPERATURE, °C
450
400
350
50
150
250
350
REACTOR VOLUME (cc)

(c)

independent variables will yield approximately the same Δ value.

The grids indicated that settings of the independent variables outside the limits of the variable space had higher Δ values. However, as pointed out in Appendix B, operation outside the limits was impossible or impractical. In some cases, higher Δ's were found for reactor volumes other than 72 cc or 340 cc, but the difference was not considered great enough to justify building other reactors.

C. Pseudo-experiments

The effect of the size of the experimental error, ε, on the convergence of the parameter estimates to their true values was considered. The values of ε were assumed to be independently and normally distributed with variance, σ_e^2, over the range of the dependent variable, ($0.006 \leq v \leq 0.085$). Three values of the standard deviation of the experimental error, σ_e, were used (σ_e = 0.0005, 0.002, 0.003).

A sequence of pseudo-experiments was conducted for each of the three σ_e's using the Δ criterion to choose the conditions for the pseudo-experiments. Hypothetical values of the dependent variable, y', were constructed for the pseudo-experiments using Model 1 and the parameter estimates ($A = 1.461 \times 10^6$, $E = 23316$, $\Theta_3 = 0.829$ and $\Theta_4 = 0.921$) to obtain calculated values of the dependent variables to which were added values of ε. Independent normal values of ε with standard deviation, σ_e, were generated by a computer subroutine. The parameters were estimated after each pseudo-experiment in each sequence and are given Table 8 (σ_e = 0.0005), Table 9 (σ_e = 0.002) and Table 10 (σ_e = 0.003).

The values of A, E and Θ_3 and Θ_4 vs. pseudo-experiment numbers for the three sequences are shown in Figures 11, 12, and 13, respectively. For

Table 8. Sequential experimental design results - σ_e = 0.0005

Pseudo-experiment Number	A* x 10^{-6}	E (cal/g mole)	Θ_3	Θ_4
5	0.0344 (± 16.8%)	22327 (± 0.3%)	0.792 (± 0.5%)	0.316 (± 10.1%)
6	2.203 (± 64.7%)	23409 (± 1.5%)	0.849 (± 5.4%)	0.964 (± 7.8%)
7	2.016 (± 28.3%)	23390 (± 1.1%)	0.843 (± 2.6%)	0.956 (± 3.3%)
8	1.559 (± 16.1%)	23251 (± 0.6%)	0.833 (± 1.7%)	0.939 (± 1.8%)
9	1.535 (± 10.8%)	23246 (± 0.5%)	0.832 (± 1.3%)	0.938 (± 1.1%)
10	1.598 (± 12.9%)	23337 (± 0.6%)	0.830 (± 1.5%)	0.935 (± 1.4%)
11	1.581 (± 12.9%)	23318 (± 0.5%)	0.831 (± 1.5%)	0.935 (± 1.4%)
12	1.550 (± 12.5%)	23278 (± 0.5%)	0.832 (± 1.5%)	0.935 (± 1.3%)
13	1.550 (± 12.5%)	23278 (± 0.5%)	0.832 (± 1.4%)	0.936 (± 1.3%)

*Dimensions of A consistent with concentrations in g moles/liter and time in sec.

Table 9. Sequential experimental design results - $\sigma_e = 0.002$

Pseudo-experiment Number	$A^* \times 10^{-6}$	E (cal/g mole)	θ_3	θ_4
5	17.588 (± 837.6%)	24138 (± 12.3%)	0.765 (± 24.2%)	1.431 (± 113.3%)
6	0.306 (± 141.4%)	23078 (± 3.4%)	0.713 (± 13.9%)	0.797 (± 20.0%)
7	1.719 (± 85.0%)	23464 (± 3.3%)	0.809 (± 8.2%)	0.959 (± 9.7%)
8	0.344 (± 63.9%)	22584 (± 2.5%)	0.742 (± 7.4%)	0.852 (± 8.0%)
9	0.387 (± 42.6%)	22608 (± 2.2%)	0.749 (± 5.5%)	0.863 (± 4.9%)
10	0.437 (± 44.1%)	22872 (± 2.1%)	0.743 (± 5.7%)	0.858 (± 5.1%)
11	0.359 (± 51.8%)	22535 (± 2.3%)	0.756 (± 6.6%)	0.851 (± 6.0%)
12	0.360 (± 48.4%)	22542 (± 2.1%)	0.756 (± 6.2%)	0.851 (± 5.6%)
13	0.350 (± 49.7%)	22515 (± 2.1%)	0.765 (± 6.2%)	0.838 (± 5.7%)

*Dimensions of A consistent with concentrations in g moles/liter and time in sec.

Table 10. Sequential experimental design results - $\sigma_e = 0.003$

Pseudo-experiment Number	$A^* \times 10^{-6}$	E (cal/g mole)	θ_3	θ_4
5	17.588 (± 837.6%)	24138 (±12.3%)	0.765 (± 24.2%)	1.431 (± 113.3%)
6	0.207 (± 141.7%)	22976 (± 3.4%)	0.707 (± 14.1%)	0.736 (± 21.5%)
7	15.807 (± 155.2%)	24006 (± 5.7%)	0.950 (± 12.9%)	1.113 (± 14.7%)
8	2.133 (± 96.1%)	22920 (± 3.3%)	0.864 (± 9.5%)	1.003 (± 10.0%)
9	1.870 (± 112.6%)	23467 (± 3.8%)	0.821 (± 11.9%)	0.952 (± 12.7%)
10	11.886 (± 113.4%)	23984 (± 4.5%)	0.922 (± 11.9%)	1.123 (± 10.1%)
11	14.976 (± 135.0%)	24689 (± 5.2%)	0.897 (± 14.7%)	1.099 (± 12.4%)
12	11.469 (± 165.6%)	23959 (± 6.2%)	0.958 (± 16.9%)	1.074 (± 15.3%)
13	12.020 (± 161.1%)	23926 (± 6.0%)	0.983 (± 15.7%)	1.059 (± 14.6%)

*Dimensions of A consistent with concentrations in g moles/liter and time in sec.

Figure 11. Frequency factor, A* vs. pseudo-experiment number

---

*Dimensions consistent with concentrations in g moles/liter and time in seconds

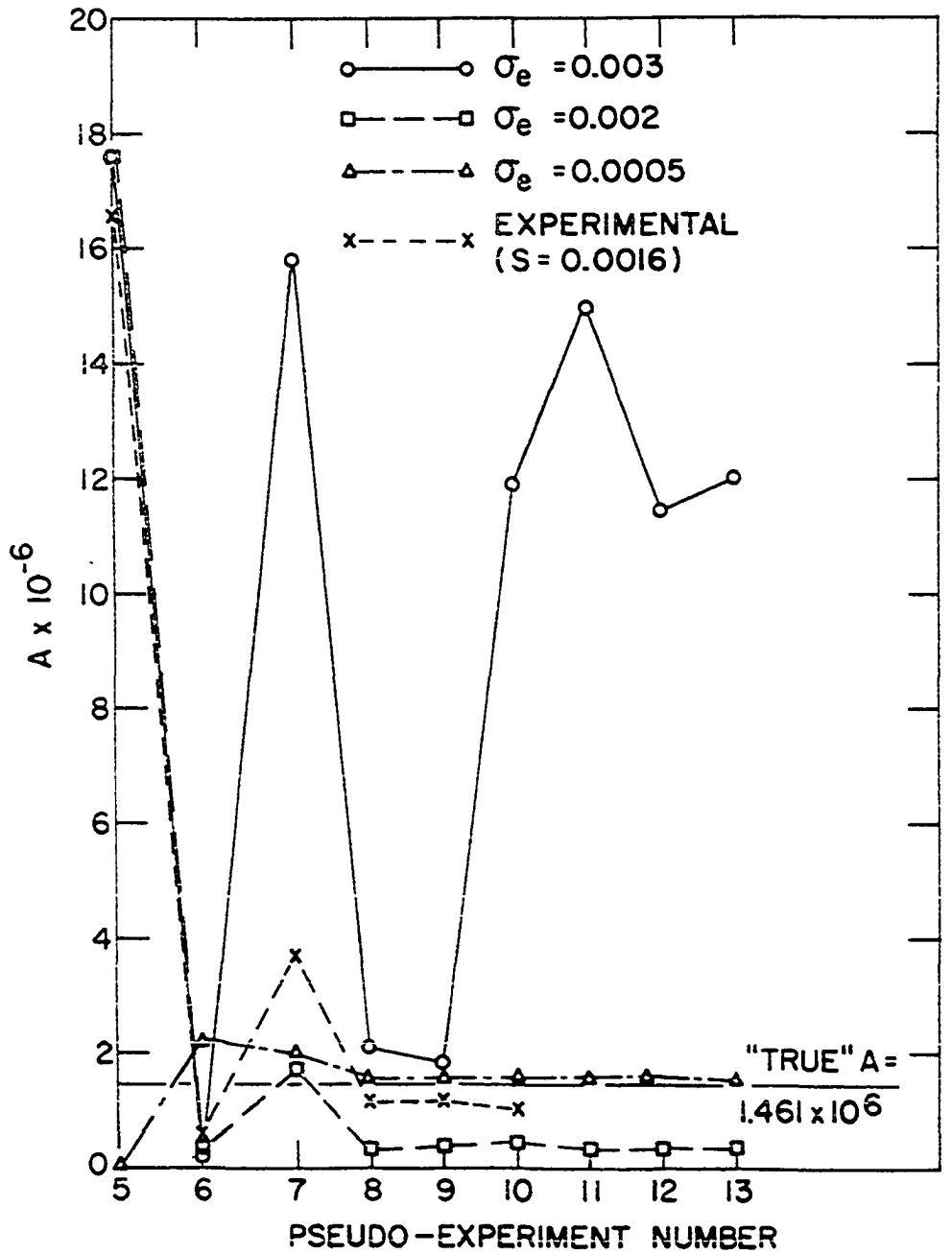
σ_e =0.003
σ_e =0.002
σ_e =0.0005
EXPERIMENTAL
(S = 0.0016)
"TRUE" A =
1.461 x 10^6
A x 10^-6
PSEUDO-EXPERIMENT NUMBER
0
2
4
6
8
10
12
14
16
18
20
5
6
7
8
9
10
11
12
13

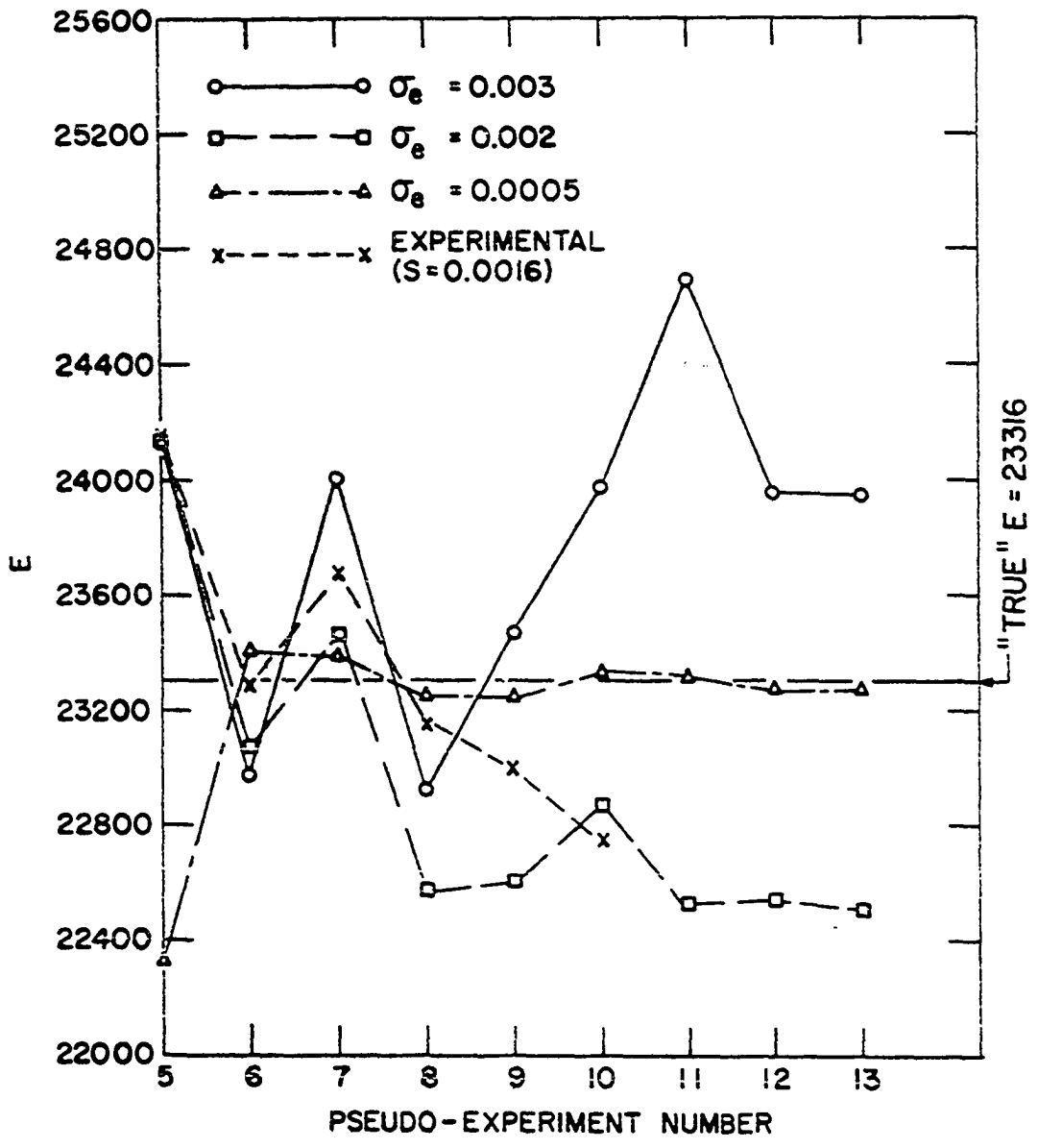

Figure 12. Activation energy E (cal/g mole) vs. pseudo-experiment number

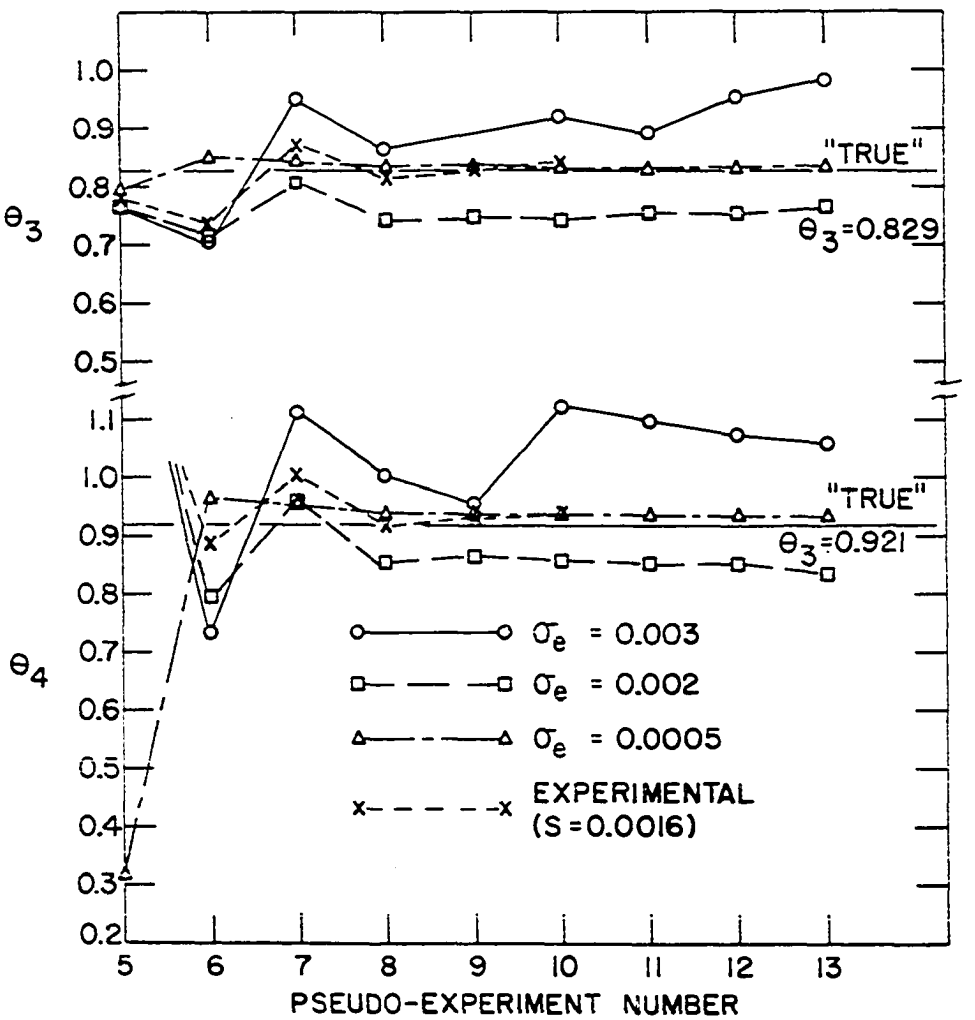

Figure 13. θ_3 and θ_4 vs. pseudo-experiment number

comparison, the parameter estimates from the sequential design of Table 6 were plotted in Figures 11, 12 and 13. In this case, Pseudo-experiment 5 corresponds to Experiment 13, Pseudo-experiment 6 corresponds to Experiment 25, etc.

When comparing the experimental results of Table 6 with the results of the pseudo-experiments, one must keep in mind that the experiments of Table 6 consist of several (generally two) replicate runs while the pseudo-experiments each consist of a single run. The effects of these replicates on the precision of the parameter estimates and rate of convergence were not determined.

Figures 11, 12 and 13 show that for σ_e = 0.0005 and 0.002, the parameter estimates converged to the final estimates in only three pseudo-experiments. For σ_e = 0.003, however, the parameter estimates fluctuated even up to the final pseudo-experiment.

It is apparent that the accuracy of the parameter estimates was less for large values of σ_e, particularly for the parameter A. For example, the ratio of the estimated value of A to the true A was 1.05, 0.25, 8.5 for σ_e = 0.0005, 0.002, 0.003, respectively. This trend was less pronounced for E, θ_3 and θ_4. For σ_e = 0.003, these estimates were within $\pm$ 20% the true values.

The experimental values for A and E in Figures 11 and 12 appear to be less than the true values. However, values of the rate constant, k, where k = A exp (-E/RT), can be nearly equal over the 350-450°C temperature range but have very different values of A and E because of the high degree of correlation between A and E. This is illustrated by Figure 14, which shows that after the eighth experiment the experimental values of k at 450°C are much more accurate than indicated by the values of A and E.

Figure 14. Rate constant, k*, at 450°C vs. Pseudo-experiment number

---

*Dimensions of k consistent with concentrations in g moles/liter and time in seconds

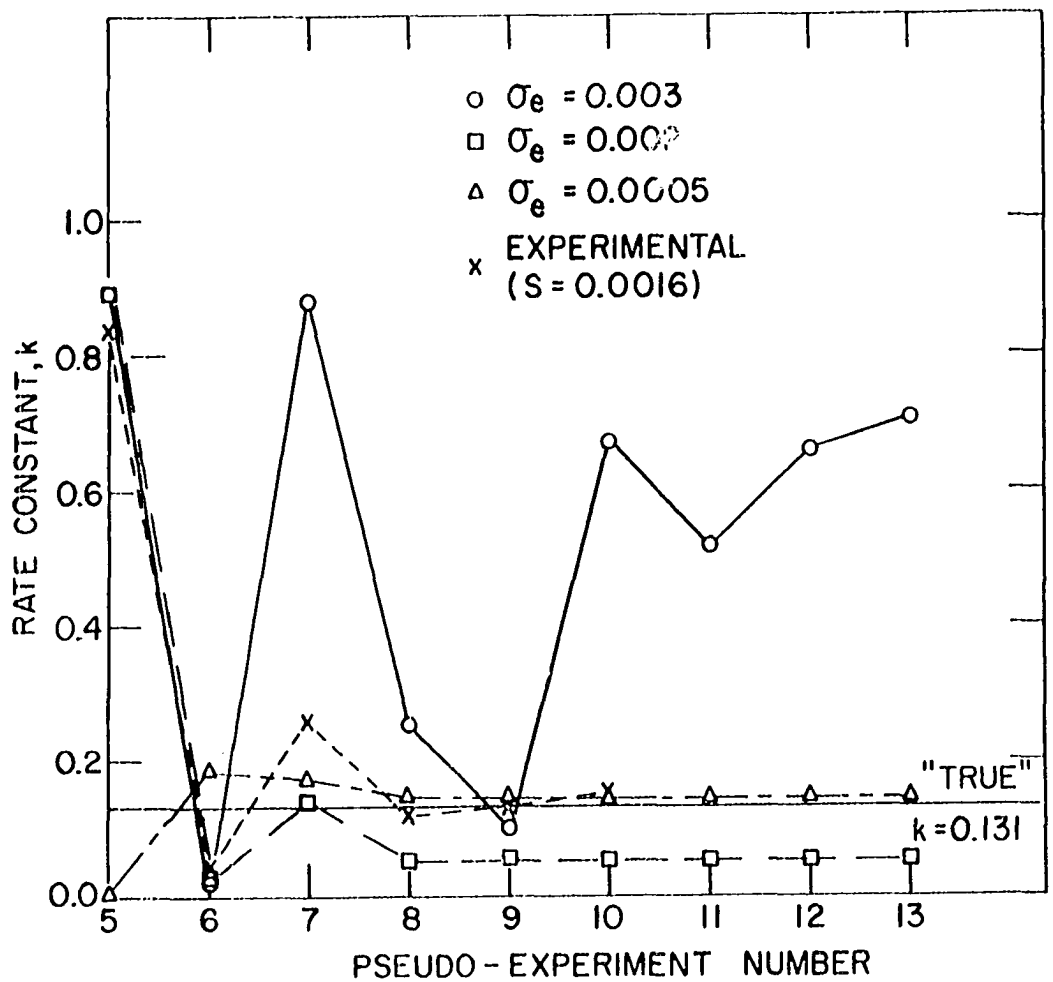
o σe = 0.003
□ σe = 0.002
Δ σe = 0.0005
x EXPERIMENTAL (S = 0.0016)
"TRUE" k = 0.131
RATE CONSTANT, k
1.0
0.8
0.6
0.4
0.2
0.0
5
6
7
8
9
10
11
12
13
PSEUDO - EXPERIMENT NUMBER

much more accurate than indicated by the values of A and E.

The volumes of the confidence regions of the parameters are roughly proportional to $\Delta^{-1/2}$. As more data are collected, the volumes of the confidence regions and $\Delta^{-1/2}$ should decrease. From Figure 15, it is apparent that $\Delta^{-1/2}$ generally does decrease with each new experiment, although after Pseudo-experiment 9 the $\Delta^{-1/2}$ values tend to level out.

The data for each pseudo-experiment consisted of one setting of the independent variables and the hypothetical dependent variable, y', (the ratio of g moles of CO_2 to g moles of Ar, CO_2 and $COCl_2$). The value of y' was calculated as the sum of $\hat{y}'$ and the independent normal error, ε, with variance, σ_e^2. The value of $\hat{y}'$ was calculated for each setting of the independent variables using Model 1 with parameters: $A = 1.461 \times 10^6$, $E = 23316$, $\theta_3 = 0.829$, $\theta_4 = 0.921$. These parameters represent the so called "true" parameters.

The Δ criterion requires a minimum of four initial experiments, so the averaged settings of the independent variables of the runs of Experiments 9-13 were used as data for the initial Pseudo-experiments 1-5. For instance, the independent variable settings of Pseudo-experiment 1 consisted of an average reactor temperature, T, an average $NbOCl_3$ concentration, C_{Ao}, etc., calculated from the data of runs 9.1, 9.2 and 9.3.

For $\sigma_e = 0.0005$, the y' values for Pseudo-experiments 1-5 were calculated as previously described using $\hat{y}'$ and ε. For $\sigma_e = 0.002$ and 0.003, y' values calculated in this manner led to convergence problems in the nonlinear parameter estimation. To avoid this problem, the y' value for Pseudo-experiment 1 for $\sigma_e = 0.002$ and 0.003 was set equal to the average experimental y value of runs 9.1, 9.2, 9.3. Likewise, the y' values of Pseudo-

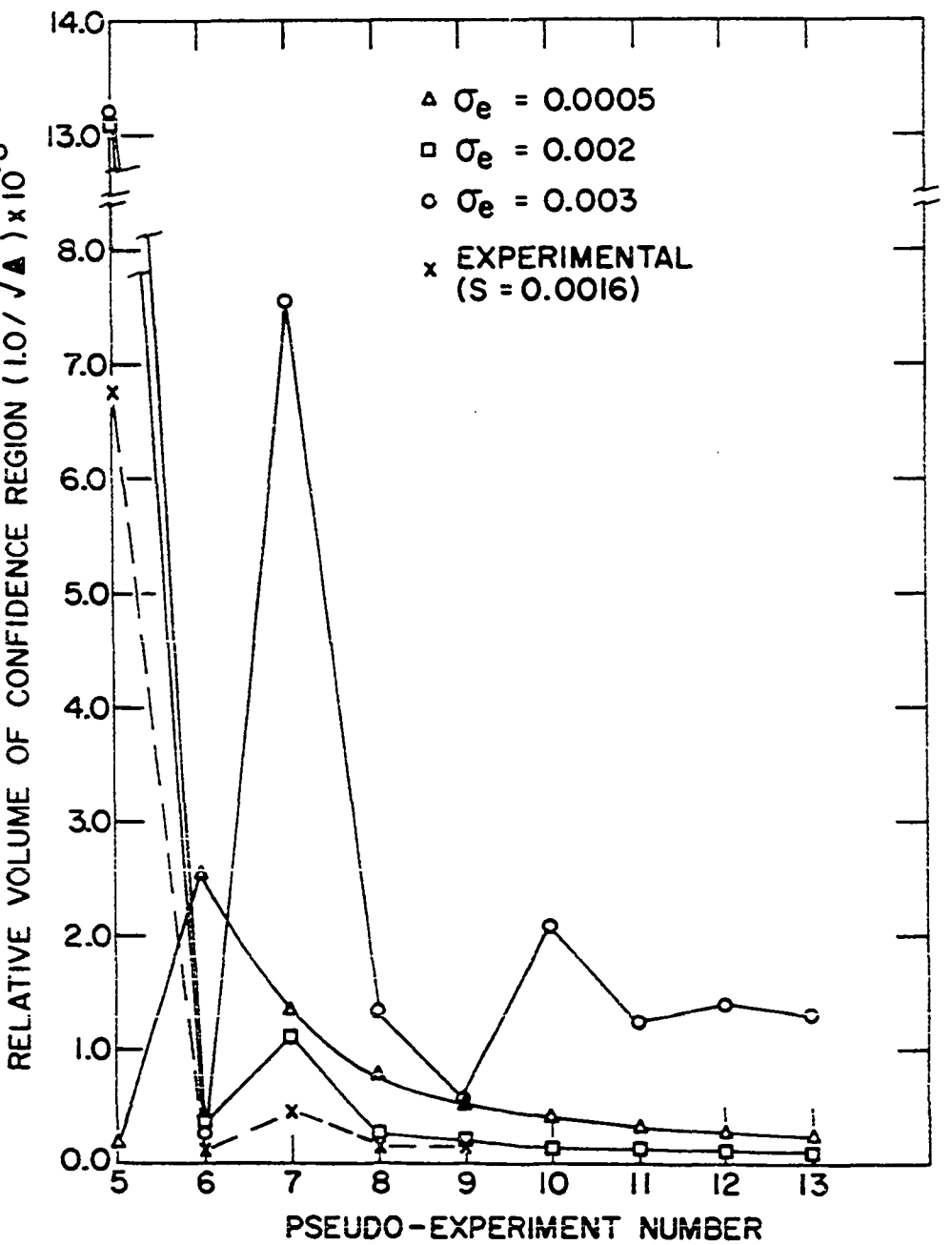

Figure 15. Relative volume of confidence region ($\Delta^{-1/2}$) vs. pseudo-experiment number

experiments 2-5 were set equal to the average experimental y values for the runs of Experiments 10-13.

The next step was to determine parameter estimates for Model 1 using the data of the initial Pseudo-experiments 1-5. Then, the Δ criterion experimental design was used to choose the settings of the independent variables for Pseudo-experiment 6 from 1536 combinations of settings of the independent variables. The experimental design was subject to the limits on the sample space, viz., $COCl_2$ decomposition, minimum CO_2 concentration, etc. Combinations of independent variables were chosen from four $NbOCl_3$ flow rates (0.04, 0.05, 0.06, 0.07 cc/sec STP), four $COCl_2$ flow rates (0.1, 0.15, 0.20, 0.25 cc/sec STP); four argon flow rates (0.1, 0.15, 0.20, 0.25 cc/sec STP); two volumes (72 cc and 340 cc); and 12 temperatures (340-460°C in 10°C increments).

A value of y' was generated for Pseudo-experiment 6 for the independent variables chosen by the Δ criterion. New parameter estimates were obtained from the data of Pseudo-experiments 1-6 and this information was used to pick the conditions for Pseudo-experiment 7 by the Δ criterion. This cycle was repeated through Pseudo-experiment 13 for each value of σ_e.

D. Errors

Eleven sets of replicate runs were made and are represented in Table 2 by the experiment numbers with the symbol (*). The runs within each set of replicates all have the same experimental number. For instance, Experiment 9 constitutes one set of replicate runs. The mean square for pure error, s_e^2, calculated from the replicate runs was 1.025×10^{-6}.

Table 11 shows how errors in such measurements as reactor pressure, reactor volume, etc. effect the value of y for runs 17.3 and 18.1. The errors

Table 11. Errors

	Measurement			% Error of y
Run 17.3 (y = 0.029)				
	Reactor Pressure (mm Hg)	= 732.7	± 1.0	+ 0.1
	Reactor Volume (cc)	= 71.7	± 1.0	+ 1.3
	Reactor Temperature (°C)	= 447.0	± 0.2	+ 0.4
	Sublimer Temperature (°C)	= 296.4	± 0.2	+ 0.6
	Argon Rate (cc/sec)	= 0.231	± 0.0035	- 1.4
	Volume of Sample (cc)	= 2.152	± 0.005	- 0.3
	Volume of CO_2 (cc)	= 0.0696	± 0.0007	+ 1.0
	Volume of $COCl_2$ (cc)	= 0.6100	± 0.0061	+ 0.2
	Volume of Cl_2 (cc)	= 0.0181	± 0.0004	+ 0.1
	Volume of Air (cc)	= 0.0077	± 0.0040	+ 0.2
Run 18.1 (y = 0.025)				
	Reactor Pressure (mm Hg)	= 738.6	± 1.0	+ 0.1
	Reactor Volume (mm Hg)	= 335.4	± 1.0	+ 0.2
	Reactor Temperature (°C)	= 352.9	± 0.2	+ 0.5
	Sublimer Temperature (°C)	= 300.2	± 0.2	+ 0.7
	Argon Rate (cc/sec)	= 0.157	± 0.0024	- 1.5
	Volume of Sample (cc)	= 2.166	± 0.005	- 0.3
	Volume of CO_2 (cc)	= 0.0568	± 0.006	+ 1.2
	Volume of $COCl_2$ (cc)	= 0.943	± 0.009	- 0.4
	Volume Cl_2 (cc)	= 0.0	± 0.0	+ 0.0
	Volume of Air (cc)	= 0.0077	± 0.004	+ 0.2

represent estimations of maximum errors for the measurements. The % error in y was calculated as follows. A value of $\hat{y}$ was calculated using Model 1, the values of the measurements, and the parameters: A = 1.46×10^6, E = 23316, Θ_3 = 0.829, Θ_4 = 0.921. Then for each measurement the positive value of the measurement error was added to the measurement and a new value of the dependent variable, $\hat{y}_e$, was calculated using Model 1 and the given parameters. The % error was calculated from the equation: % error = $(\hat{y}-\hat{y}_e)\ 100/\hat{y}$. For example, a + 0.005 cc error in measurement of the sample volume would cause a - 0.3% error in y for run 17.3 of Table 11.

E. $COCl_2$ Decomposition

Ten to twenty times more $COCl_2$ decomposition was encountered in some experiments than was predicted by the thermal decomposition rate equation (Equation 8), suggesting the possibility of a catalytic reaction. The absence of light did not seem to affect the rate of decomposition and the thermal decomposition equation (Equation 8) did not fit the data. In Experiments 14, 20, 26 and 27 and run 17.2 the Cl_2 from the decomposition interferred with the CO_2 measurement to such an extent that the data of these experiments were not used. $COCl_2$ decomposition occurred to a lesser extent (less than 1 mole per cent Cl_2 in the sample) in Experiments 16, 23 and 28 and runs 17.3 and 25.2. For these experiments, a linear correction was made for the $COCl_2$ decomposition.

Special cleaning of the reactor was attempted using 20-30% NaOH solution, which reduced the $COCl_2$ decomposition for Experiments 21-25. However, by Experiments 26 and 27, the $COCl_2$ decomposition was again high despite the special cleaning. The problem was resolved by using a new reactor which resulted in only slight $COCl_2$ decomposition in Experiments 28 and 29.

VII. DISCUSSION OF RESULTS

A. Model Discrimination and Parameter Estimation

Based on a comparison of the sum of squares of the residuals and the F test, the general rate expression, Model 1, appears best to correlate the kinetic data. However, Models 2 and 3, representing the elementary rate expression and a transistion intermediate rate expression, respectively, could not be rejected on the basis of the statistical evidence. All attempts to fit other models to the data were unsuccessful because of lack of fit or physically unrealistic parameters. It is apparent from Figure 2 that there are no outliers in the data set for Model 1 and all of the $\hat{y}$ vs. y points are of the 45° line; roughly 70% being within one standard error of y.

Figure 5a, the plot of the residuals vs. the extent of the conversion as represented by y, showed no reason to doubt the assumption of a normally and independently distributed error with zero mean. The plots of the residuals vs. other pertinent variables showed no significant trends. The residual plots made after each experiment and the statistical tests showed no reason for rejecting Model 1 at any stage.

The mean square for pure error, $s_e^2 = 1.025 \times 10^{-6}$, represents an estimate of the lower limit of the pure or experimental error variance because the replicates were not replicates in the true sense. That is, all independent variables were not independently reset for each run as is required for true replicates. This is discussed in more detail in part C of this section. Since this low value of s_e^2 occurs in the denominator of the F ratios represented in Table 3, the values of the ratios, which vary between 7.4 and 10.5, are higher than one would expect for true replicates. Con-

sequently, the lack of fit indicated by the F ratio at the 95% confidence limit (F = 2.27) is considered to have little significance.

Discrimination between Models 1, 2 and 3 is probably not possible because the variable space of this work was not great enough to reveal major inadequacies of the models and minor differences were masked by the experimental error. This problem can be illustrated by comparing Models 2 and 3. At 350°C, Model 3 has the same form as Model 2 because the denominator of the rate equation of Model 3 is essentially 1.0 at this temperature. Furthermore, since the rate constants, k, are 0.0461 and 0.0409 for Models 2 and 3, repsectively, differences in the predicted conversions of the models would be obscured by the experimental error (roughly by 5-10% of y). At 450°C, however, the denominator of the rate equation of Model 3 is proportional to the $NbOCl_3$ concentration and is in the range of 0.1 to 2.0. This indicates that data taken at higher temperatures and higher $NbOCl_3$ concentrations would be useful in discriminating between these models. Development of an experimental technique with a much lower experimental error would be another alternative.

Comparison of the areas of the 95% confidence regions of Figures 6 and 7 might lead to the conclusion that the Λ criterion experimental design gives more precise estimates than the unplanned approach. The comparison is not straight forward, however, because a large experimental error could also account for differences in the size of the confidence regions. Boesiger's (7) estimate of the standard error of y due to pure error, s_e, was 0.0245 based on only three replicates which is clearly much greater than s_e value of 0.00101 of this work. The scatter of Boesiger's $\hat{y}$ vs. y data of Figure 3 also suggests Boesiger's experimental error was greater

than the experimental error of this work, assuming Model 1 is adequate. Therefore, it is impossible to determine how much of the difference in the sizes of the confidence region is due to the experimental design and how much is due to differences in the experimental errors of the two works.

Boesiger (7) also found that Model 1 gave the best fit for his data. However, Boesiger's parameters predicted $\hat{v}$ values that are consistently lower than the $\hat{v}$ values predicted by the parameters of this work (See Figure 4). The differences in the results of the two studies are too great to be explained by errors of measurement of the variables. The explanation must be in some source of error that is not subject to quantitative analysis. For instance, incomplete mixing in the batch reactors might be one reason for Boesiger's low conversions.

B. Experimental Design

Rapid convergence seems to be an attribute of the Δ criterion as long as the experimental error is not too great. This is illustrated by the results in Table 5. After the initial experiments, only three experiments were required for convergence of the estimates to within approximately one standard error of the "true" parameters. Again, in Figures 11, 12 and 13 only three pseudo-experiments were required for convergence for σ_e = 0.0005.

As one might expect, for large experimental errors, the parameter estimates either do not converge rapidly or do not converge at all. For σ_e = 0.002, although the estimates converge after only three Δ criterion experiments, the estimates do not converge to the true values. For σ_e = 0.003 the estimates do not converge at all.

While the settings of the independent variables for the maximum Λ are desirable, the settings which yield large values of Λ also appear to cause rapid convergence. The results of Table 7 show that though the Λ's for the experiments in the sequence 25-28-23-18-19 were smaller than the maximum Λ's, the convergence of the parameter estimates in Table 6 was still rapid.

The precision of the parameter estimates, as measured by the estimated standard errors of the parameters and the relative volumes of the confidence regions, reached a limit after the first three Δ criterion experiments. Subsequent experiments did not improve the precision.

In general, the estimated standard errors of the parameters were reduced by each succeeding experiment until the third Δ criterion experiment. After this experiment, the standard errors were not reduced by more experiments. This is illustrated by the results in Tables 6, 8, 9 and 10.

The relative volumes of the confidence regions also decreased rapidly for the first three experiments of the Δ criterion sequence (Pseudo-experiments 6, 7 and 8). After Pseudo-experiment 8, however, the relative volumes did not decrease significantly with each subsequent experiment.

The Δ criterion was not too useful in choosing the settings of the independent variables after three or four Λ criterion experiments. The results of Table 7 illustrate this statement. After Experiments 9-13 the maximum Λ value was 180 times the minimum Λ indicating that certain settings of the independent variables were definietly superior. By the fourth experiment chosen by the Δ criterion, (Experiment 18) the maximum Δ was only 1.67 times as large as the minimum Δ. This means that a great many settings of the independent variables would satisfy the Δ criterion and that

the choice of the conditions for the next experiment was not very important from the standpoint of the Λ criterion.

In theory, the Δ criterion could be used to pick the conditions for the initial experiments. However, this is usually impractical because the first estimates of the parameters are generally poor and the independent variable space is not well defined. In addition, the limitations on the experimental equipment are often not known.

For these reasons, the initial experiments should be used to explore the independent variable space and to test the limits of the equipment. The initial Experiments 9-13 were not used in this manner, however. Little information was obtained on the upper limits of the capacity of the condensers until Experiments 16 and 17. The condenser limitations should have been determined in the first two or three experiments. Furthermore, the estimates of the parameters determined by the data of Experiments 9-13 were inaccurate because the range of the $COCl_2$ concentrations was too small. These poor initial parameter estimates, however, did not interfere with the rapid convergence of the Δ criterion design.

In retrospect, only four initial experiments plus three or four Λ criterion experiments would have been sufficient for estimating the parameters of Model 1. On completion of the eighth experiment, the parameter estimates would converge and subsequent experiments would not improve the estimates. In addition, the Δ surfaces would have leveled out and the Δ criterion would no longer be useful in choosing the conditions for the next experiment.

This would be a logical stopping point if Model 1 were known to be the true model and if the experimental error were known. However, some experi-

ments should be conducted to test Model 1 and for replications to estimate the experimental error. There are no rules for determining how many replicates are required or whether the model has been adequately tested. The number of these experiments is arbitrary, but in any case the total number of experiments would not be significantly less than the 16 experiments of this study.

C. Errors

The size of the experimental error greatly affected the accuracy of the estimates. Figures 11, 12 and 13 show that accurate estimates were obtained for small standard deviations of the experimental error, viz., $\sigma_e = 0.0005$. For $\sigma_e = 0.002$ and $\sigma_e = 0.003$, however, the estimates were poor. For example, the rate constants, k, calculated using the final parameter estimates for $\sigma_e = 0.002$ were 60-70% lower than the "true" rate constants in the range 350-450°C. For $\sigma_e = 0.003$, the rate constants using the final estimates were ten times greater than the "true" rate constants. The size of σ_e had less influence on θ_3 and θ_4 than on A and E. Even for $\sigma_e = 0.003$, θ_3 and θ_4 were within 20% of the "true" parameters, whereas the estimate of A was 8.5 times the true value. This suggests that the order of reaction could be estimated approximately even for large experimental errors.

The relative precision of the estimates were strongly influenced by the size of σ_e. For instance, the final standard errors of A were 12.5%, 49.7% and 161.7% for $\sigma_e = 0.0005$, 0.002 and 0.003 respectively.

For genuine replicate runs, the entire set of conditions for a run must be reset anew, preferably after intermediate runs at other settings.

Although the flow rates were reset for the replicates of Table 2, the reactor temperature and sublimer temperature were not, and no intermediate runs were conducted between replicates. Therefore, the replicates of Table 2 are something less than genuine replicates. Consequently, the value of 1.025×10^{-6} calculated for the mean square of the pure error, s_e^2, should be considered as an estimate of the lower limit of s_e^2.

Experiments 11, 13 and 22 and Experiments 21 and 23 were attempts to obtain sets of replicate runs. These attempts were unsuccessful because the independent variable settings could not be duplicated due to difficulties in resetting the salt bath temperatures and flow rates and to changes in the reactor volumes caused by breakage and replacement.

The value of the standard error of y due to pure error, s_e, is a measure of the precision of the experimental y values. If the experimental error were normally and independently distributed with zero mean over the range of y values (0.006 to 0.085), then s_e could be taken as an estimate of the standard deviation of the experimental error.

The true value of s_e was estimated to lie in the range 0.00101 to 0.00210, where the lower limit was calculated from the value of s_e^2 (1.025×10^{-6}) estimated from the replicate runs. The upper limit was taken as the value of the standard error of y, s (0.00210), of Model 1 for lack of a better estimate. This assumption is supported by Figures 11, 12 and 13. These figures indicate that the estimates of the parameters from the sequence of real experiments of Table 6 were more accurate than the estimates for $\sigma_e = 0.002$ but less accurate than the estimates when $\sigma_e = 0.0005$. The real experiments generally consisted of two replicate runs while each pseudo-experiment consisted of only a single run; however, the effect of

replicates on the values of the parameter estimates is not great. For instance, the estimates of A, E, θ_3 and θ_4 using the average conditions of the runs for each of the Experiments 9-13 were 17.6×10^6, 24138, 0.765 and 1.431, respectively, while for the data of all the runs of the Experiments 9-13 the estimates of A, E, θ_3 and θ_4 were 16.6×10^6, 24143, 0.784 and 1.388.

The results of Table 11 show how errors in measurement effect y. The largest source of error for run 17.3 was 1.3% and was the result of the error in measurement of the reactor volume. This was only 0.2% for the large reactor of run 18.1. Although the reactor volume can be measured very accurately from inlet to outlet, the uncertainty arises because some reaction occurs in part of the condenser (roughly the first 2 cc). In addition, part of the reactor (about 1 cc) extends above the level of the salt, and consequently is at a lower temperature than the salt bath. These two errors tend to negate each other, however. The volume for the constant temperature reaction was taken as the volume of the reactor between inlet and outlet. The maximum error in volume due to this approximation was assumed to be about 1.0 cc.

Even though the argon flow rate was measured very accurately ($\pm$ 1.5%) by the mass flowmeters, this error was important (about 1.5% of y). The argon flow rate was also used in calculating the $NbOCl_3$ flow rate and the $COCl_2$ flow rate.

Small errors in temperature measurement produced large errors in y. A 0.2°C error in the reactor temperature caused 0.4-0.5% error in y and 0.2% error in the sublimer temperature caused 0.6-0.7% error in y.

The measurement of the CO_2 volume in the sample was also an important

source error (1.0-1.3%). Other errors in measurement caused errors of less than 0.3% in y.

One such source of error was in the method of calculating the flow rate of $NbOCl_3$. The assumption was made that the argon was saturated in the sublimer with $NbOCl_3$ according to Gloor's (20) vapor pressure equations. The flow rate of $NbOCl_3$ was therefore dependent on the argon rate. The magnitude of the error introduced by calculating the $NbOCl_3$ flow rate in this manner cannot be estimated precisely. However, as Table 1 of part IV shows, flow rates estimated using this method were within $\pm$ 5% of the measured flow rates. An error of 5% in the $NbOCl_3$ flow rate would cause a 4% error in y. This error was an upper limit because the method used to measure the $NbOCl_3$ flow rates of Table 1 was not very accurate.

Another source of error was in the assumption involved in the initial equilibrium $NbCl_5$ concentration resulting from the decomposition of $NbOCl_3$ in the sublimer. Again, Gloor's (20) vapor pressure equations were used to estimate the extent of the decomposition. Since the decomposition of $NbOCl_3$ was slight, an error of 100% in the initial equilibrium $NbCl_5$ concentration causes only a 1.7% error in y.

VIII. CONCLUSIONS

1. The kinetic data of this work for the chlorination of $NbOCl_3$ with $COCl_2$ was correlated best by the empirical rate equation:

$$dC_A/dt = -A \exp(-E/RT)\, C_A^{\Theta_3} C_B^{\Theta_4}$$

where:

C_A, C_B = concentrations of $NbOCl_3$ and $COCl_2$, g moles/liter, respectively

t = reaction time, sec

T = reaction temperature, °K

The best estimates of the parameters, determined by nonlinear least squares analysis, were $A = 1.461 \times 10^6$, $E = 23316$ cal/g mole, $\Theta_3 = 0.829$ and $\Theta_4 = 0.921$. The units of A are consistent with dC_A/dt expressed in g moles/liter sec. The experimental data were obtained at low $NbOCl_3$ concentrations (less than 20 mole %) for the temperature range 340-450°C essentially at atmospheric pressure.

2. The parameter estimates obtained in this work are considerably more precise than Boesiger's (7) parameter estimates. However, the parameter estimates were highly correlated, particularly A and E. More precise parameter estimates could only be obtained by reducing the experimental error or extending the variable space to include a greater range of concentrations and temperatures. This is beyond the scope of the equipment used in this work.

3. The use of the Δ criterion experimental design leads to rapid convergence of the parameter estimates if the model is adequate and if the experimental error is not too great. The accuracy and rate of convergence of the parameter estimates are very sensitive to the size of the experimental

error. The upper limit of the standard deviation of the experimental error, σ_e, for accurate estimates and rapid convergence was estimated to be in the range 0.001 to 0.002 for the conditions of this work where y values varied between 0.006 and 0.085.

4. The iterative cycle based on the Δ criterion was particularly suited to this study because the experiments were difficult and time consuming. The rapid convergence which led to precise estimates in only three Δ criterion experiments was the most attractive feature. Also, the examination of the results after each experiment was useful in assuring that no major inadequacy of the model would go undiscovered for a large number of experiments.

IX. RECOMMENDATIONS

Extending the upper temperature and space time limits to conditions where significant $COCl_2$ decomposition occurs could provide more data for accurate parameter estimates and model discrimination. Accurate analysis of CO, Cl_2, CO_2, $COCl_2$ and the carrier gas would be required, but a dual column chromatographic technique could possibly be developed.

The influence of the size of the experimental error and the size of the variable space on the ability to discriminate between kinetic models has not been clearly established. Some insight into this problem could be obtained by using the computer to simulate data after the manner described for the pseudo-experiments of this work. In this way, the accuracy required of the data for model discrimination could be determined. Likewise, for data with a given accuracy, the range of the variable space necessary for model discrimination could be established. This information would be useful for evaluating experimental techniques for further work on the chlorination of $NbOCl_3$ with $COCl_2$.

Perhaps a generalized method could be developed for evaluating the ability of an experimental technique to furnish data which would be suitable for model discrimination. This would require reasonably accurate preliminary information on the models and parameters, knowledge of the expected experimental error of the technique, and the general bounds of the variable space.

The apparent catalytic $COCl_2$ decomposition encountered in some of the experiments of this work was not fully investigated. Excessive $COCl_2$ decomposition due to catalysts might be a problem in other applications of $COCl_2$ as a chlorinating agent. Further research in this area appears to be useful.

X. BIBLIOGRAPHY

1. Atkinson, A. C. Statistical designs for pilot-plant and laboratory experiments. Part I. Chemical Engineering 73: 149-154. May 9, 1966.

2. Beale, E. M. L. Confidence regions in non-linear estimation. Roval Statistical Society Journal, Part B, 22: 41-75. 1960.

3. Behnken, D. W. Estimation of copolymer reactivity ratios: an example of non-linear estimation. Journal of Polymer Science, Part A, 2: 645-668. 1964.

4. Bodenstein, M., Brenschede, W. and Schumacher, H. J. Die photochemische Phosgenbildung. XI. Zeitschift fur Physikalishe Chemie B40: 121-134. 1938. Original available but not translated; translated by Sharon K. Myers, Ames Laboratory, U.S. A.E.C. 1966.

5. Bodenstein, M. and Plaut, H. Bildung und Zerfall von Phosgen in der Warme. Zeitschrift fur Physikalishe Chemie 110: 399-416. 1924. Original available but not translated; translated by Sharon K. Myers, Ames Laboratory, U.S. A.E.C. 1966.

6. Boesiger, D. D. Kinetics of the vapor phase chlorination of niobium oxytrichloride using carbonyl chloride. Unpublished Ph.D. thesis. Ames, Iowa, Library, Iowa State University. 1967.

7. Boesiger, D. D. and Stevenson, F. D. Kinetics of the vapor phase chlorination of niobium-oxychloride by phosgene. To be published Metallurgical Transactions ca. 1970.

8. Box, G. E. P. Fitting empirical data. New York Academy of Sciences Annals 86: 792-816. 1960.

9. Box, G. E. P. Use of statistical methods in the elucidation of basid mechanisms. Institute of International Statistics Bulletin 36: 215-225. 1957.

10. Box, G. E. P. and Hunter, W. G. The experimental study of physical mechanisms. Technometrics 7: 23-42. 1965.

11. Box, G. E. P. and Hunter, W. G. A useful method for model building. Technometrics 4: 301-318. 1962.

12. Box, G. E. P. and Lucas, H. L. Design of experiments in non-linear situations. Biometrika 46: 77-90. 1959.

13. Brothers, J. A. Process for preconditioning the carbon bed used in a method of converting refractory metal clorides. U.S. Patent 3,128,150. April 7, 1964.

14. Cleland, F. A. and Wilhelm, R. H. Diffusion and reaction in viscous-flow tubular reactor. American Institute of Chemical Engineers Journal 2: 489-497. 1956.

15. Christiansen, J. A. Über den thermischen Zerfall des Phosgens. Zeitschrift fur Physikalishe Chemie 103: 99-138. 1922. Original available but not translated; translated by David J. Lorine, Ames Laboratory, U.S. A.E.C. 1965.

16. Draper, N. R. and Smith, H. Applied regression analysis. New York, N.Y., John Wiley and Sons, Inc. 1966.

17. Dunn, W. E. Chlorination of niobium oxychloride. U.S. Patent 3,009,773. November 21, 1961.

18. Dunn, W. E. Process for converting niobium oxychloride to niobium pentachloride. U.S. Patent 3,107,144. October 15, 1963.

19. Elger, G. W. and Boubel, R. W. Production of hafnium metal. U.S. Patent 3,971,549. January 1, 1963.

20. Gloor, M. and Weiland, K. Thermal and optical investigation of vapors of niobium oxychloride ($NbOCl_3$) (Translated title). Helvetica Chimica Acta 44: 1098-1120. 1961. Original available but not translated; translated by Elly Korthoven, Ames Laboratory, U.S. A.E.C. 1967.

21. Hart, W. and Meyer, G. The system $NbCl_5$-Nb_2O_5. II. The P-T projection. Recueil des Travaux Chimiques des Pays-Bas: 1233-1246. 1964.

22. Hart, W. and Meyer, G. The system $NbCl_5$-Nb_2O_5. III. The equilibrium constant of the equilibrium $5\ NbOCl_3 \rightleftarrows 3\ NbCl_{5_g} + Nb_2O_5$. Recueil des Travaux Chimiques des Pays-Bas 84: 1155-1165. 1965.

23. Hart, W. and Meyer, G. The system $NbCl_5$-Nb_2O_5. IV. The T-x projection. Recueil des Travaux Chimiques des Pays-Bas 83: 1233-1246. 1967.

24. Huber, K. and Baunok, I. Uberzwei neue Oxidichloride des 5-wertigen Niobs. Chimial 5: 365-366. 1961. Original available but not translated; translated by Wayne N. Svoboda, Ames, Laboratory, U.S. A.E.C. 1966.

25. Hunter, W. G. and Atkinson, A. C. Statistical designs for pilot-plant and laboratory experiments. Part II. Chemical Engineering 73: 159-168. June 6, 1966.

26. Hunter, W. G., Kittrell, J. R. and Mezaki, R. Experimental strategies for mechanistic modeling. Institute of Chemical Engineers Transactions 45: T146-T152. 1967.

27. Jere, G. V., Patel, C. C. and Krishnan, V. Thermodynamic considerations in the chlorination of different oxides constituting columbite and tantalite. Metallurgical Society of the American Institute of Mechanical Engineers Transactions 221: 866-873. 1961.

28. Kittrell, J. R., Hunter, W. G. and Watson, C. C. Non-linear least squares analysis of catalytic rate models. American Institute of Chemical Engineers Journal 11: 1051-1057. 1965.

29. Kittrell, J. R., Hunter, W. G. and Watson, C. C. Obtaining precise parameter estimates for non-linear catalytic rate models. American Institute of Chemical Engineers Journal 12: 5-10. 1966.

30. Kittrell, J. R., Mezaki, R., and Watson, C. C. Estimation of parameters for non-linear least squares analysis. Industrial and Engineering Chemistry 57, No. 12: 19-27. December 1965.

31. Kittrell, J. R., Mezaki, R. and Watson, C. C. Model-building techniques for heterogenous kinetics. British Chemical Engineering 11, No. 1: 15-19. January 1966.

32. Kowalczyk, K. J. Kinetic study of the thermal formation and dissociation of phosgene in a tubular reactor. Unpublished M.S. thesis. Ames, Iowa, Library, Iowa State University. 1967.

33. Lapidus, L. and Peterson, T. I. Analysis of heterogenous catalytic reactions by non-linear estimation. American Institute of Chemical Engineers Journal 11: 891-897. 1965.

34. Levenspiel, O. Chemical reaction engineering. New York, N.Y., John Wiley and Sons, Inc. 1962.

35. Marquardt, D. W. An algorithm for least-squares estimation of non-linear parameters. Industrial and Applied Mathematics Society 11: 431-441. June 1963.

36. Meyer, G., Oosterom, J. R. and Van Oeveren, W. J. The system $NbCl_5$-Nb_2O_5. Recueil des Travaux Chimiques des Pays-Bas 80: 502-508. 1961.

37. Mezaki, R. and Kittrell, J. R. Parametric sensitivity in fitting non-linear kinetic models. Industrial and Engineering Chemistry 59, No. 5: 63-69. May 1967.

38. Nisel'son, L. A. Separation and purification of niobium and tantalum by distillation of their pentachlorides. Russian Journal of Inorganic Chemistry 3: 14-32. 1958.

39. Peterson, T. I. Kinetics and mechanisms of napthalene oxidation by non-linear estimation. Chemical Engineering Science 17: 203-219. 1962.

40. Peterson, T. I. Reaction kinetics optimization using non-linear estimation. Chemical Engineering Progress Symposium Series 56, No. 31: 111-120. 1960.

41. Peterson, T. I. and Lapidus, L. Non-linear estimation analysis of the kinetics of catalytic ethanol dehydrogenation. Chemical Engineering Science 21: 655-664. 1966.

42. Saeki, Y., Suzuki, T., and Matsushima, T. Thermodynamical properties of niobium oxychloride. Electrical Society of Japan Journal 32: 143-147. 1964.

43. Schafer, H. and Kahlenberg, F. Bildungsenthalpie, Sattigungsdruek und Thermochemisches Verhalten des Nioboxychlorids $NbOCl_3$. Zeitschrift fur Anorganishe und Allgemeine Chemie 305: 327-340. 1960. Original available but not translated; translated by M. J. Watts, Risley, England.

44. Shchukarev, S. A., Smirnova, E. K., Shcmyakina, T. S. and Rvabor, E. N. Hydrolysis and enthalpy of formation of niobium oxide trichloride. Russian Journal of Inorganic Chemistry 7: 626-628. 1962.

45. Stranks, D. R. Kinetics of isotope exchange reactions. Part 6. The thermal carbon monoxide and phosgene system. Faraday Society Transactions 51: 524-527. 1955.

XI. ACKNOWLEDGEMENTS

The author wished to acknowledge his appreciation to Dr. F. D. Stevenson for his assistance and advice throughout this work.

Also, the author would like to call special attention to the work done by Dwight Boesiger which laid the ground work for this study.

Special thanks are also given to Harvey Jensen for his help in building and maintaining the equipment, especially when "catastrophes" occurred.

Steve Michalicek and Scott Haigh, research helpers, deserve commendation for their long hours and hard work.

XII. APPENDIX A

A. Thermal Decomposition of $NbOCl_3$

The primary reaction for the thermal decomposition of $NbOCl_3$ is:

$$5\ NbOCl_3\ (g) \rightleftarrows 3\ NbCl_5\ (g) + Nb_2O_5\ (s)$$

This equilibrium has been studied by a number of researchers (20, 21, 22, 36, 42, 43).

The results of these investigations agree well on the total equilibrium vapor pressure and the vapor pressure of $NbOCl_3$, but there is considerable disagreement on the equilibrium concentration of $NbCl_5$ vapor. Table 12 summarizes the equilibrium mole per cent of $NbCl_5$ at temperatures in the range 260-320°C estimated from the vapor pressure equations of three researchers. All agree that the equilibrium $NbCl_5$ mole per cent is low (1-7%) at temperatures less than 300°C. At temperatures over 300°C, Saeki's (42) data predicts considerably more decomposition of the $NbOCl_3$ than the data of Gloor (20) or Schafer (43).

Saeki's results are supported by the vapor pressure equations of Hart and Meyer (22) which predict 9-10 mole per cent $NbCl_5$ at 300-320°C. However, Hart and Meyer's vapor pressure equations were for the range 340-400°C and extrapolation to lower temperatures may not be valid. To avoid the uncertainty in the extent of $NbOCl_3$ decomposition at high temperatures, the temperatures used to sublime $NbOCl_3$ for this study were 300°C or less.

In this study the decomposition of $NbOCl_3$ appeared to be slight at temperatures below 300°C as evidenced by the appearance of only trace quantities of yellow $NbCl_5$ crystals in the collection tubes during the $NbOCl_3$ flow rate measurement. Also no evidence was found of thermal decomposition of $NbOCl_3$ (i.e. white deposits of Nb_2O_5) on the walls of the connector tube.

These observations tend to agree qualitatively with Gloor (20) and Schafer (43), who found that the thermal decomposition of $NbOCl_3$ vapor amounted to only a few per cent and that the amount of thermal decomposition decreased or remained constant with increasing temperature.

Table 12. Equilibrium mole per cent of $NbCl_5$ in the vapor phase for the system $NbCl_5(g) - NbOCl_3(g) - Nb_2O_5(s)$

Temperature (°C)	$NbCl_5$ (Mole %) Gloor's Data (20)	$NbCl_5$ (Mole %) Saeki's Data (42)	$NbCl_5$ (Mole %) Schafer's Data (43)
260	3.40	0	0
270	2.98	3.76	0
280	2.59	4.64	1.27
290	2.29	5.15	1.30
300	2.01	6.91	1.33
310	1.79	8.29	1.40
320	1.59	9.80	1.40

Although the extent of the decomposition of $NbOCl_3$ appears to be slight, it is necessary to take this decomposition into account. This was done by assuming the vapor entering the reactor was at the equilibrium composition determined by the sublimer temperature. The equilibrium vapor pressure equations of Gloor (20) were used to estimate this equilibrium composition.

The vapor pressure equations of Gloor were used because his findings

agreed qualitatively with the findings of this study. Also, Gloor's measurements of the equilibrium $NbCl_5$ concentrations were probably the most reliable. Gloor's data were obtained directly by spectrophotometric measurement in the temperature range 270-300°C that was used in this study. The other researchers (21, 22, 36, 42) estimated the $NbCl_5$ concentrations indirectly by vapor pressure measurements.

Since no kinetic data exists on the thermal decomposition of $NbOCl_3$, it is not possible to show the validity of the assumption of equilibrium of the system $NbOCl_3(g)$ - $NbCl_5(g)$ - $Nb_2O_5(s)$ in the sublimer. Saeki (42), however, states that the system reaches equilibrium within one hour or less. In any case, the correction appears to be in the right direction and since the correction is small, a fairly large error in the assumption of equilibrium would not be too serious.

Other minor products are known to occur when $NbOCl_3$ is sublimed. The presence of blue-black crystals, possibly Nb_3O_7Cl, has been reported as a residue after the sublimation of $NbOCl_3$ (23, 36, 43). Shchukarev (44) found a powdery grey residue of Nb_4O_9Cl after subliming $NbOCl_3$. Huber (24) reported NbO_2Cl formed as a light grey loose sublimate when $NbOCl_3$ was sublimed in an evacuated sealed tube at 350°C. Gloor (20) and Schafer (43) however, state that they were unable to demonstrate a compound having this composition. Hart and Meyer (23) found that NbO_2Cl does not exist in the temperature range 200-430°C, but they were unable to establish the occurrence or nonoccurrence of Nb_3O_7Cl and $Nb_4O_9Cl_2$ with any certainty. These materials are found in trace quantities and for practical purposes the side reactions that form them can be assumed to be negligible.

B. Thermal Decomposition of $COCl_2$

The reaction:

$$COCl_2(g) \underset{k_f}{\overset{k_d}{\rightleftharpoons}} CO(g) + Cl_2(g)$$

has been studied by a number of investigators (4, 5, 15, 32) and the parameters for the kinetic equation have been estimated.

The most commonly accepted expression for the rate equation is:

$$dC_{COCl_2}/dt = -k_d C_{COCl_2} C_{Cl_2}^{1/2} + k_f C_{CO} C_{Cl_2}^{3/2} \qquad (8)$$

where:

C_{COCl_2}, C_{Cl_2}, and C_{CO} = concentrations of $COCl_2$, Cl_2 and CO, respectively in g moles/liter

t = residence time, seconds

Kowalczyk (32) recently estimated the following expressions for k_d and k_f:

$$k_d = 3.332 \times 10^{12} \exp(-4.958 \times 10^4/RT)$$

$$k_f = 6.216 \times 10^7 \exp(-2.524 \times 10^4/RT)$$

To avoid problems presented by the $COCl_2$ decomposition, runs were made at conditions where Equation 8 with Kowalczyck's values of k_d and k_f predicted less than 0.1% decomposition.

XIII. APPENDIX B

Plug Flow Assumption

Cleland and Wilhelm (14) studied the effect on conversion of radial diffusion and radial distribution of reaction times in viscious-flow tubular reactors. They showed that plug flow conversions were approached when:

$$\alpha\lambda = \mathcal{D}\, V/2R^2v > 1.0$$

where:

$\mathcal{D}$ = molecular diffusivity, cm^2/sec

V = volume of reactor, cc

R = reactor tube radius, cm

v = volumetric flow rate at reactor conditions, cc/sec

$\alpha\lambda$ = dimensionless group

Levenspeil (34) considered the case of a fluid in plug flow, on top of which was superimposed some degree of back mixing or intermixing. Deviations from plug flow were correlated with the dimensionless group, D/uL, where D is a parameter related to the axial dispersion with units of cm^2/sec, u is the average velocity in the reactor, cm/sec, and L is the length of the reactor. For streamline flow in pipes, D can be calculated as follows:

$$D = u^2R^2/48$$

provided $uR/\mathcal{D} \ll 7.5L/R$

Using this relationship for D, the dimensionless group, D/uL, can be related to Cleland and Wilhelms criterion as follows:

$$D/uL = R^2v/48\mathcal{D}V$$

or $$D/uL = 1/96\alpha\lambda$$

Levenspeil (34) estimated that the maximum error in using the plug flow assumption, when $D/uL = 0.01$, is 0.5%. The maximum D/uL for this study was estimated to be 0.00012 while the minimum $\alpha\lambda$ was 90. Clearly by either criterion, the plug flow assumption was reasonable for the conditions of this work.

XIV. APPENDIX C

Nonlinear Estimation of Parameters

Consider the u^{th} experiment of a total of N experiments. For brevity let $\vec{\xi}_u$ represent the vector of the independent variable settings. Let $\vec{\rho}$ be the vector of the estimated parameters A, E, Θ_3, Θ_4. Then, the predicted response, $\hat{y}_u$ can be represented by a function of $\vec{\xi}_u$ and $\vec{\rho}$.

$$\hat{y}_u = f(\vec{\xi}_u, \vec{\rho}) \tag{9}$$

The relationship between the observed response, y_u, and predicted response, $\hat{y}_u$ is:

$$y_u - \hat{y}_u = \varepsilon_u \qquad u = 1,2,3...N$$

where ε_u is termed the u^{th} residual. If $f(\vec{\xi}_u, \vec{\rho})$ is the true functional relationship, then ε_u is simply the experimental error.

The problem now is to find the values of $\vec{\rho}$ which produce the predicted response, $\hat{y}_u$, which best approximates the observed response, y_u. The criterion used to determine these parameters is known as the least squares criterion. This criterion is satisfied by choosing the values of $\vec{\rho}$ which minimize the sum of squares of the residual, $S(\rho)$, where:

$$S(\rho) = \sum_{u=1}^{N} (y_u - \hat{y}_u)^2 \quad . \tag{10}$$

If the assumption is made that the errors are distributed independently and normally with identical variance, the least squares parameter estimates are also the maximum likelihood estimates. One further assumption that is made is that the errors of setting and determining the independent variables are negligible.

At this point, it is necessary to consider reparameterization of A and E. When the sum of squares surface defined by Equation 10 contains contours that are long and attenuated, slow convergence of any iterative process is likely (8). This sort of "ill condition" has been found to take place when the equation for $\hat{y}_u$ contains an exponential dependence on temperature, such as the Arrenhius equation:

$$k = A \exp -E/RT \quad .$$

As Box (8) noted, reparameterization can be accomplished by redefining the temperature variable so that the center of its coordinate system is near the center of the experimental design. This is done if the specific rate constant, k, is redefined by:

$$k = \theta_1 \exp [-\theta_2(1/T-1/\bar{T})]$$

where:

$$\bar{T} = \frac{T_1 + T_2 \ldots + T_u \ldots + T_N}{N}$$

$$\theta_1 = A \exp -E/R\bar{T}$$

$$\theta_2 = E/R$$

After reparameterization:

$$\hat{y}_u = f(\vec{\xi}_u, \vec{\theta})$$

$$S(\theta) = \sum_{u=1}^{N} (y_u - \hat{y}_u)^2$$

where $\vec{\theta}$ is the vector θ_1, θ_2, θ_3, θ_4.

If $f(\vec{\xi}_u, \vec{\theta})$ were a linear expression, then linear least squares techniques could be used to solve for $\vec{\theta}$. This would be done by taking the partial derivatives of S(0) with respect to the θ_i's and setting these partial derivatives equal to zero. This precedure would yield a set

of simultaneous equations which could be readily solved. However, $f(\vec{\xi}_u,\vec{\theta})$ is nonlinear in the parameters and the set of simultaneous equations can only be solved by numerical techniques. Consequently an algorithm known as the Gauss method will be used to solve these equations.

To aid in the explanations in other sections, the Gauss method will be briefly outlined. Let $\vec{\theta}^{(o)}$ represent the vector of initial parameter estimates. Let p represent the total number of parameters. Expanding $f(\vec{\xi}_u,\vec{\theta})$ in a Taylor's series and retaining only the first terms results in:

$$f(\vec{\xi}_u,\vec{\theta}) = f(\vec{\xi}_u,\vec{\theta}^{(o)}) + \sum_{j=1}^{p} (\theta_j-\theta_j^{(o)})\left[\frac{\partial f(\vec{\xi}_u,\vec{\theta})}{\partial\theta_j}\right]_{\vec{\theta}=\vec{\theta}^{(o)}} . \qquad (11)$$

For brevity let:

$$Z_u = y_u - f(\vec{\xi}_u,\vec{\theta}^{(o)}) \qquad (12)$$

$$\beta_j = \theta_j - \theta_j^{(o)} \qquad (13)$$

$$g_{uj} = \left[\frac{\partial f(\vec{\xi}_u,\vec{\theta})}{\partial\theta_j}\right]_{\vec{\theta}=\vec{\theta}^{(o)}} . \qquad (14)$$

When Equations 11, 12, 13, 14 are substituted in Equation 9 the result is:

$$Z_u = \sum_{j=1}^{p} g_{uj}\beta_j + \varepsilon_u . \qquad (15)$$

Note that Equation 15 is linear and the β_j's can now be found by the standard linear least squares method. Thus the β_j's are found by solving for B in Equation 16:

$$(G^TG)\vec{B} = \vec{G}^T\vec{Z} . \qquad (16)$$

$$\underset{\sim}{G} = \begin{bmatrix} g_{11} & g_{12} & \cdots & g_{1p} \\ g_{21} & g_{22} & \cdots & g_{2p} \\ \vdots & & & \\ g_{N1} & g_{N2} & \cdots & g_{Np} \end{bmatrix}$$

$$\underset{\sim}{B} = \begin{bmatrix} \beta_1 \\ \beta_2 \\ \vdots \\ \beta_p \end{bmatrix}$$

$$\underset{\sim}{Z} = \begin{bmatrix} Z_1 \\ Z_2 \\ \vdots \\ Z_N \end{bmatrix}$$

$\vec{B}$ is termed the correction vector. The value of $\theta_j^{(1)}$ for the next iteration is:

$$\theta_j^{(1)} = \beta_j + \theta_j^{(o)} \qquad j = 1,2...p \quad .$$

The procedure can then be repeated until the corrections become small - that is, until the procedure converges.

The primary disadvantage of the Gauss method is that the initial estimates of $\vec{\theta}$ must be in the neighborhood of the best parameter estimates, $\hat{\theta}$, for convergence. However, this disadvantage can be overcome to some extent by scaling the initial corrections, β_j, by factors as great as 100. The scale factor can be reduced with each succeeding iteration. This generally leads to convergence of the method in 15 iterations or less.

XV. APPENDIX D

Adequacy of Fit and Precision

Perhaps the most common test of adequacy of fit is the mean square about the regression, s^2, defined by the equation:

$$s^2 = S(\hat{\theta})/(N-p)$$

where $S(\hat{\theta})$ is the minimum sum of squares; N is the total number of experiments; and p is the number of parameters. The value of s^2 will be greater for an inadequate model than for the true model. This criterion has been used to discriminate between various kinetic models (33, 39, 40).

Another means of judging the adequacy of fit of a model is by comparing the mean square due to lack of fit, s'^2 with the mean square for the pure error, s_e^2, where:

$$s'^2 = \frac{S(\hat{\theta}) - s_e^2 \sum_{i=1}^{m} (R_i - 1)}{N-p - \sum_{i=1}^{m} (R_i - 1)}$$

and

$$s_e^2 = \frac{\sum_{i=1}^{m} \sum_{j=1}^{R_i} (y_{ij} - \bar{y}_j)}{\sum_{i=1}^{m} (R_i - 1)}$$

where:

m = the total number of groups of replications

R_i = the number of replications in group i

y_{ij} = the j^{th} observed response in the i^{th} group

$\bar{y}_j$ = the arithmetic average of y_{ij}'s in the i^{th} group of replications.

The value of s'^2 will not be significantly different from s_e^2 if the model is adequate (8,9). The lack of fit is tested by comparing the ratio of s'^2/s_e^2 with the $100(1 - \alpha)$% point of an F distribution having

$$N - p - \sum_{i=1}^{m} (R_i - 1) \text{ and } \sum_{i=1}^{m} (R_i - 1) \quad \text{degrees of freedom.}$$

The quantities s^2 and s_e^2, provide independent estimates of the variance, σ^2, of y if there is no lack of fit.

The analysis of the residuals, where the u^{th} residual, ε_u, is defined as:

$$\varepsilon_u = y_u - \hat{y}_u$$

is perhaps the most powerful method of determining the adequacy of fit. The residuals can reveal both the extent and nature of the inadequacy of a model. Draper and Smith (16) and Box (9) suggest various ways in which the residuals can be plotted. For instance, the residuals might be plotted against:

(1) the predicted response, y_u

(2) the level of each of the independent variables

(3) the time order in which the experiments were performed.

These plots could reveal whether the residual is related to the value of the response; whether the model fails to take the variables properly into account; or whether there are time trends in the results.

In addition to the adequacy of fit, some estimate of the precision of the parameters is necessary. Many of the results developed for the linear case cannot be rigorously applied to nonlinear problems. However, approximate estimates of the confidence intervals and the confidence regions can

be obtained by applying linear theory to the nonlinear case (9).

The standard errors may be approximated for the individual parameters by:

$$s(\theta_j) = (C_{jj}s^2)^{1/2} \qquad j = 1,2...p$$

where $s(\theta_j)$ is the estimated standard error of the j^{th} parameter, and C_{jj} is the j^{th} diagonal of the $(G^TG)^{-1}$ matrix defined in Appendix C. This relation is true to the extent that the Taylor expansion of $f(\vec{\xi}_u,\vec{\theta})$ represents the predicted response surface for y_u in the vicinity of the nonlinear least square estimates.

The confidence region of the parameter estimates can be defined by:

$$S(\theta) = S(\hat{\theta})[1 + \frac{p}{N-p} F(p, N-p, 1-\alpha)] \qquad (17)$$

where:

$S(\hat{\theta})$ = the minimum value of the sum of squares

p = the number of parameters

N = the number of experimental points

$F(p, N-p, 1-\alpha)$ = the F distribution with p and N-p degrees of freedom at the α significance level.

Two dimensional plots of $S(\theta)$ as a function of θ_i and θ_j can be prepared holding the other parameters constant at say their minimum sum of squares estimates. To apply Equation 17 one must calculate the sums of squares of enough sets of parameter values to establish a locus of $S(\theta)$ equal to the right hand side of Equation 17. This locus provides an approximate 100 $(1-\alpha)$ per cent confidence region for the parameters.

If the equation for $\hat{y}_u$ were linear with respect to its parameters such a region would be elliptical. Since the equation is nonlinear, the

region will not be elliptical and its deviation from an elliptical shape is a measure of the nonlinearity of the model. The shape of these regions can show high correlations between the parameters and show up poor experimental design (10).

XVI. APPENDIX E

Range of Independent Variables

One of the first steps in planning the experiment was to determine ranges for the independent variables. In some cases these limits were determined precisely by clear limitations of the experimental equipment. In others, the limits were not clear and were chosen arbitrarily. Occasionally these limits had to be extended or reduced after initial experiments were made.

The limits on five independent variables, two limits imposed by equipment considerations, and two limits imposed by decomposition of the reactants were set. These limits with the reasons for chosing them are listed as follows:

1. Reactor Temperature

Boesiger (6) noted that the reaction rate was negligible at temperatures lower than 340°C. Therefore, the lower temperature limit was set at 340°C. The upper limit was set at 460°C because the $COCl_2$ decomposition was too great at higher temperatures.

2. Reactor Volume

Calculations using Boesiger's (7) parameters and the parameters determined in this study indicated that the reactor volume should not be less than 50 cc because of low conversions at smaller volumes. Experience has shown that reactors larger than 350 cc are bulky and difficult to handle. These two considerations set the volume range between 50 cc and 350 cc.

Reactor volumes of 70 cc and 340 cc were arbitrarily chosen. As discussed in the results, the experimental design indicated that there would be no advantage in using other volumes in the 50-350 cc range.

3. Argon and $COCl_2$ Flow Rates

The minimum flow rate for argon and $COCl_2$ that can be determined accurately is about 0.10 cc/sec STP. The initial upper limit was set arbitrarily at 1 cc/sec. Later, it was found that flow rates larger than 0.4 cc/sec were not worth considering because the resulting space times were too low for sufficient conversion. Hence, the flow rate range was set at 0.1-0.4 cc STP.

4. $NbOCl_3$ Flow Rate

The minimum $NbOCl_3$ flow rate was set at 0.01 cc/sec. Lower flow rates result in low CO_2 concentrations that cannot be measured accurately.

The maximum flow rates were set at 0.07 cc/sec for the 70 cc reactor and 0.06 cc/sec for the 340 cc reactor. The choice of these limits was based on (1) the amount of time required for the concentration of the gases at the sampling tee to reach steady state, and (2) the amount of time the condenser can operate before plugging.

The time required for steady state was determined by measuring the concentration of the gas with a Gow-Mac detector placed at the sampling tee. The largest time required for the gas concentration at the sampling tee to reach steady state was 13 minutes. With this figure in mind plus an arbitrary safety factor of two minutes a limit of 15 minutes was set for holding the independent variables constant before taking a sample. In a similar manner, the limit for the 70 cc reactor was set at 10 minutes.

By trial and error, it was found that the condensers would take 0.4-0.5 grams of $NbOCl_3$ before plugging. For the 340 cc reactor, this set the maximum $NbOCl_3$ rate at about 0.06 cc/sec STP to allow for 15 minutes of

steady state operation. For the 70 cc reactor, a maximum $NbOCl_3$ rate of 0.07 cc/sec STP allowed the required 10 minutes of steady state operation.

It might seem that to achieve greater $NbOCl_3$ rates, one should simply build a larger condenser. However, a larger condenser requires more time to reach steady state. This tends to defeat the original purpose, so that the net effect would be to increase the $NbOCl_3$ rate only slightly or not at all.

The condenser was designed mainly by trial and error. Admittedly, the condenser might be improved to allow higher $NbOCl_3$ rates, but the effort required would be considerable and the chances of success doubtful.

The problems in designing an effective condenser to remove the $NbOCl_3$ and $NbCl_5$ are considerable. First, the condenser should have as little volume as possible to keep the time required for steady state small. But, freshly condensed $NbOCl_3$ is a fluffy material with a density of only 0.01-0.02 gm/cc. This means that 50-100 cc are required for each gram of $NbOCl_3$ that condenses. Since $NbOCl_3$ is so light, the flow velocity in the condenser must be low to prevent entrainment.

In addition, the $NbCl_5$ has a much higher vapor pressure than $NbOCl_3$ and therefore condenses at temperatures about 100°C lower than $NbOCl_3$. Therefore space is required in the condenser for cooling the $NbCl_5$ vapor and collecting the condensed $NbCl_5$.

5. Minimum CO_2 Concentration

The minimum CO_2 concentration that could readily be measured accurately was around 0.8 volume %. Therefore 0.8% was established as the lower allowable limit for the CO_2 concentration. Modification of the chromatographic procedure would have allowed lower CO_2 concentrations to be

measured, but the experimental design indicated that this was not necessary.

6. Maximum Space Time

An arbitrary limit of 9 minutes was set for the space time. This limit was set because of the difficulty in holding the independent variables at constant values for longer space times.

7. Thermal Decomposition of $COCl_2$

Although the maximum limit on the reactor temperature of 460°C was chosen because of the $COCl_2$ decomposition, some combinations of the flow rates and reactor volumes led to $COCl_2$ decomposition at temperatures less than 460°C. Equation 8 and the parameters estimated by Kowalczyk (32) were used to estimate the $COCl_2$ decomposition at these conditions. The maximum allowable limit on the $COCl_2$ decomposition was set at 0.1 mole per cent.

8. Thermal Decomposition of $NbOCl_3$

A limit of 300°C was set for the maximum temperature of the sublimer to prevent the possibility of high $NbOCl_3$ decomposition (See Appendix A).

XVII. APPENDIX F

A. Preliminary Procedure

1. The sublimer was loaded with 5-8 grams $NbOCl_3$ in a dry box. The inlet and outlets of the sublimer were sealed with corks and the sublimer was stored in a dry box until just before use.

2. The controllers of the salt bath heaters were set to bring the salt bath temperatures within 5°C of the desired operating temperatures. This was done 10-12 hours before the start of the run to allow the salt bath temperatures to come to steady state. Minor adjustments were made several hours before the run to bring the salt bath temperatures to within ± 1°C of the desired operating temperatures.

3. Calibration curves for CO_2 and $COCl_2$ (See Appendix G), were generally made on the day before the run, the day of the run, or the day following the run. When it became apparent that there was little or no change in the calibration curves with time, the calibration curves were made less frequently. However, in all cases the calibration curves were made within two weeks of the run.

4. The silica gel of the chromatograph column was dryed for two hours at 200°C several hours before the run. After the column had been cooled to the normal operating temperature of 30°C, a 2.5 cc sample of $COCl_2$ was injected into the column. If CO_2 was detected (from the reaction of $COCl_2$ and water adsorbed on the silica gel), the silica gel was dryed at 200°C for another hour. Again $COCl_2$ was injected into the column. This procedure was repeated until no CO_2 was observed.

5. The mass flowmeters were turned on several hours before the start of the run in order to warm up the electronic components of the flowmeters.

A calibration curve was made for the argon mass flowmeter either immediately before the start of the run or immediately after the end of a run. The mass flowmeter was calibrated using a 10 cc soap film flowmeter.

6. The argon purge stream was started several hours before the run to purge the reactor and lines of air.

B. Run Procedure

1. When the salt bath temperatures appeared to be at steady state the sublimer was mounted in the small salt bath.

2. The system was tested for leaks by plugging the condenser outlet, setting the system pressure at 10 cm of glycerine, and checking to see if this pressure remained constant for at least 5 minutes.

3. An argon gas stream was allowed to flow through the sublimer at a low rate (0.05 cc/sec). A second argon stream was maintained at 0.1 - 0.15 cc/sec through the $COCl_2$ inlet line to the reactor.

4. After the sublimer had been in place one to two hours, the condenser was removed and replaced by a clean condenser.

5. The $COCl_2$ was turned on and the flow rate was adjusted to the desired level. The argon flow rate was also adjusted to the proper rate at this point.

6. The following information was recorded every five minutes:

   a. small salt bath temperature (millivolts)

   b. large salt bath temperature (millivolts)

   c. the $COCl_2$ flowmeter reading (Volts or scale reading depending on whether mass flowmeter or rotameter were used)

   d. the argon flowmeter reading (Volts)

   e. pressure drop through system (cm of glycerine)

   f. clock time

7. Every 15-20 minutes the helium carrier gas rates on both chromatograph columns were measured with a soap film flowmeter. The ambient temperature was also measured at this time.

8. The ambient pressure was recorded at the beginning of the run and checked every one to two hours.

9. The controller settings on both salt baths and the mass flowmeter readings at zero flow rate were recorded.

10. Bridge current, detector temperature and the column temperature of the chromatograph were recorded.

11. After the system had been running at steady state for 15-20 minutes, a sample was withdrawn from the exit gas line with a 2.5 cc syringe and injected into the chromatograph. The chromatograph was operated as described in Appendix G. The attenuation used for each of the sample's components and the time of the sample were recorded.

12. After the sample had been taken, the $COCl_2$ was shut off and the argon purge was turned on and adjusted to 0.1 cc/sec. The argon flow through the sublimer was reduced to 0.05 cc/sec. The chromatograph temperature was cooled to 30°C by a stream of high pressure air. This cooling procedure required about 30 minutes.

13. If a second sample was needed, the condenser was replaced and steps 4 through 11 were repeated.

14. At the end of the experiment the reactor was purged with air or dry helium.

XVIII. APPENDIX G

Operation of the Chromatograph

The chromatograph used in this study was a Model 720 dual column programmed temperature gas chromatograph with nickel detector cell filaments manufactured by F & M Scientific Corporation. The column consists of 5 in. of F & M A-40 silica gel (30-60 mesh) in a 6-in. long, 1/8-in. O.D. column. The silica gel was activated at 150°C for 3 hours in a stream of helium. The flow rate of the helium carrier gas was maintained at 20.5 cc/min STP by a flow controller. The detector temperature was maintained at 45°C with a bridge current of 190 mA. The chart speed used was 1 in./min. The column temperature could be held at any temperature up to 500°C by an insulated oven with a heater and a blower to circulate the air.

The attenuation used depended on the quantity and the kind of gas in the gas sample. Typical attenuations for $COCl_2$ and CO_2 for various sample volumes are listed in Table 13. Calibration curves were made for CO_2 and $COCl_2$ at the attenuations required for analysis of the gas samples.

The $COCl_2$ calibration data were obtained by injecting measured sample volumes into the chromatograph by means of a syringe. The column was held at 30°C for the first 3 minutes after injecting the sample. The column temperature was then raised to 150°C to elute the $COCl_2$. This was done by setting the temperature control of the oven to 150°C. About 2 minutes were required for the column temperature to reach 150°C.

A linear plot was made of sample volume vs. peak area, as determined by a disc integrator (See Figure 16). The standard deviation of the residuals for the plot was 0.006 cc or approximately 0.5% of the response.

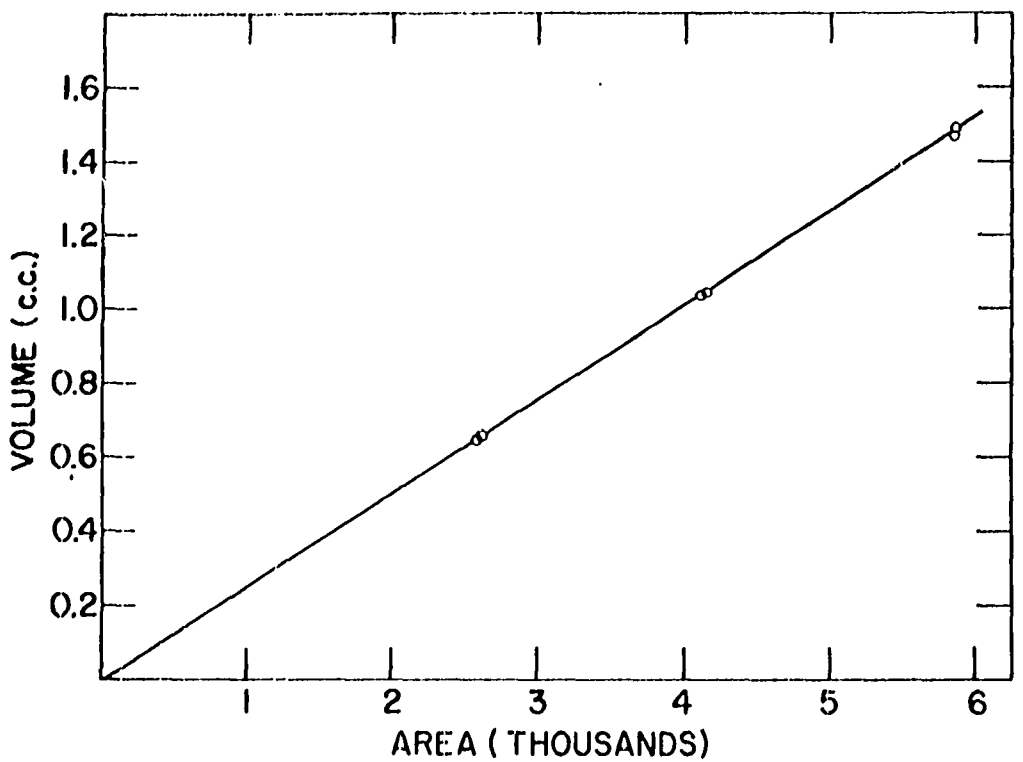

Figure 16. $COCl_2$ calibration curve - $COCl_2$ volume vs. peak area

Table 13. Chromatograph attenuations for various gas sample volumes

Gas	Range of Gas Volume in Sample	Attenuation
CO_2	0.10 cc - 0.22 cc	8
CO_2	0.05 cc - 0.15 cc	4
CO_2	0.03 cc - 0.075 cc	2
CO_2	0.015 cc - 0.04 cc	1
$COCl_2$	0.5 cc - 2.0 cc	64
$COCl_2$	0.10 cc - 1.0 cc	32

The CO_2 calibration curves were made in the normal way by injecting CO_2 samples into the chromatograph by means of a syringe. The column temperature was held at 30°C.

Samples of the gases from the reactor were taken with a 2.5 cc syringe and injected into the chromatograph. The chromatograph was operated in the same manner as described for the $COCl_2$ calibration data. A typical chromatogram is presented in Figure 17 showing the analysis of a 2.5 cc sample containing 33% argon, 2% CO_2 and 65% $COCl_2$. Retention times for the argon, CO_2, and $COCl_2$ were approximately 20, 100, and 400 sec, respectively, for the conditions as described. (Chlorine, in similar mixtures, was eluted at about 270 sec with some interference with the $COCl_2$ peak. A 1 in. longer silica gel column should result in satisfactory resolution of chlorine). Determination of concentrations was made from calibration curves for CO_2 and $COCl_2$. The argon concentration was determined by the difference between the sample volume and the sum of the carbon dioxide and

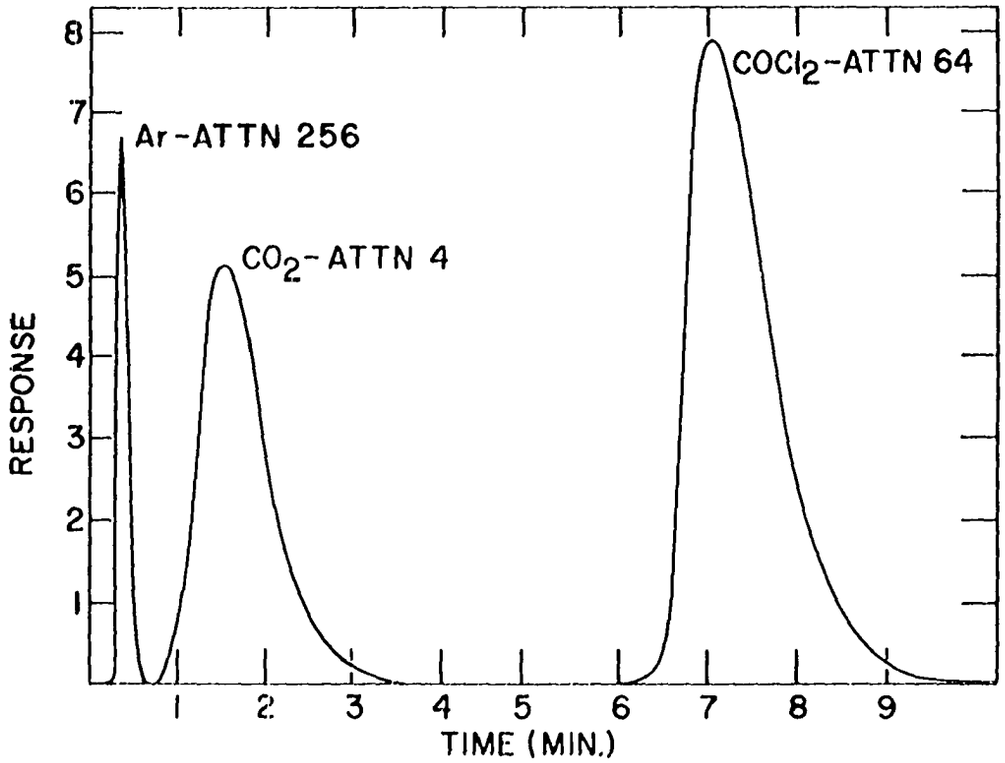

Figure 17. Chromatogram of Ar, CO_2 and $COCl_2$ (sample volume 2.5 cc)

$COCl_2$ volumes.

Initially calibration curves were made within one day of the run, because it was suspected that the calibration curves might change with use due to the corrosive properties of $COCl_2$. Comparison of the curves showed no change, however. When a composite $COCl_2$ calibration curve was made with three sets of data taken at two week intervals, the standard deviation was 0.0177 cc or approximately 1.5% of the response. Minor differences between data sets were probably the result of minor differences in the setting of the detector bridge current and carrier gas flow rate.